Fish and Shellfish Immunology 142 (2023) 109099

Contents lists available at ScienceDirect

Fish and Shellfish Immunology

journal homepage: www.elsevier.com/locate/fsi

Full length article

Antibacterial and anticancer activity of two NK-lysin-derived peptides from the Antarctic teleost *Trematomus bernacchii*

F. Buonocore [a], P.R. Saraceni [a,b], A.R. Taddei [c], A. Miccoli [d], F. Porcelli [a], S. Borocci [a,e], M. Gerdol [f], F. Bugli [g,h], M. Sanguinetti [g,h], A.M. Fausto [a], G. Scapigliati [a], S. Picchietti [a,*]

[a] *Dept. for Innovation in Biological, Agro-food and Forest systems (DIBAF), University of Tuscia, Largo dell'Università snc, 01100, Viterbo, Italy*
[b] *Italian National Agency for New Technologies, Energy and Sustainable Development (ENEA), Division of Health Protection Technologies, 00123, Rome, Italy*
[c] *Center of Large Equipments, Section of Electron Microscopy, University of Tuscia, Largo dell'Università Snc, 01100, Viterbo, Italy*
[d] *National Research Council, Inst. for Marine Biological Resources and Biotechnology, 60125, Ancona, Italy*
[e] *National Research Council, Inst. for Biological Systems (ISB-CNR) Secondary Office of Rome-Reaction Mechanisms c/o Department of Chemistry, Sapienza University of Rome, P.le A. Moro 5, 00185, Rome, Italy*
[f] *Dept. of Life Sciences, University of Trieste, 34127, Trieste, Italy*
[g] *Dept. of Basic Biotechnological Sciences, Intensive and Perioperative Clinics, Catholic University of the Sacred Heart, Rome, 00168, Italy*
[h] *Dept. of Laboratory Sciences and Infectious Diseases, A. Gemelli University Hospital Foundation IRCCS, 00168, Rome, Italy*

ARTICLE INFO

Keywords:
Antimicrobial peptides
NK-lysin
Enterococcus faecalis
Acinetobacter baumannii
Melanoma cells
Trematomus bernacchii

ABSTRACT

The NK-lysin antimicrobial peptide, first identified in mammals, possesses both antibacterial and cytotoxic activity against cancer cell lines. Homologue peptides isolated from different fish species have been examined for their functional characteristics in the last few years. In this study, a NK-lysin transcript was identified *in silico* from the head kidney transcriptome of the Antarctic teleost *Trematomus bernacchii*. The corresponding amino acid sequence, slightly longer than NK-lysins of other fish species, contains six cysteine residues that in mammalian counterparts form three disulphide bridges. Real time-PCR analysis indicated its predominant expression in *T. bernacchii* immune-related organs and tissues, with greatest mRNA abundance detected in gills and spleen. Instead of focusing on the full *T. bernacchii* derived NK-lysin mature molecule, we selected a 27 amino acid residue peptide (named NKL-WT), corresponding to the potent antibiotic NK-2 sequence found in human NK-lysin. Moreover, we designed a mutant peptide (named NKL-MUT) in which two alanine residues substitute the two cysteines found in the NKL-WT. The two peptides were obtained by solid phase organic synthesis to investigate their functional features. NKL-WT and NKL-MUT displayed antibacterial activity against the human pathogenic bacterium *Enterococcus faecalis* and the ESKAPE pathogen *Acinetobacter baumannii*, respectively. Moreover, at the determined Minimum Inhibitory Concentration and Minimum Bactericidal Concentration values against these pathogens, both peptides showed high selectivity as they did not exhibit any haemolytic activity on erythrocytes or cytotoxic activity against mammalian primary cell lines. Finally, the NKL-MUT selectively triggers the killing of the melanoma cell line B16F10 by means of a pro-apoptotic pathway at a concentration range in which no effects were found in normal mammalian cell lines. In conclusion, the two peptides could be considered as promising candidates in the fight against antibiotic resistance and tumour proliferative action, and also be used as innovative adjuvants, either to decrease chemotherapy side effects or to enhance anticancer drug activity.

Abbreviations: AMP, Antimicrobial peptide; **NKL-WT**, NK-lysin wild type peptide; **NKL-MUT**, NK-lysin mutant peptide; **MIC**, Minimum Inhibitory Concentration; **MBC**, Minimum Bactericidal Concentration; **PBS**, saline phosphate buffer; **ANS**, 1-aminonaphtalene-8-sulfonic acid; **DMEM**, Dulbecco's Modified Eagle Medium; **FCS**, fetal calf serum; **ATP**, adenosine triphosphate; **TUNEL**, Terminal Deoxynucleotidyl-Transferase mediated dUTP Nick End Labeling; **MD**, molecular dynamics; **PE**, zwitterionic phosphatidylethanolamine; **PG**, phosphatidylglycerol.

* Corresponding author. Department for Innovation in Biological, Agro-food and Forest systems, University of Tuscia, Largo dell'Università, I-01100 Viterbo, Italy.
E-mail address: picchietti@unitus.it (S. Picchietti).

https://doi.org/10.1016/j.fsi.2023.109099
Received 18 July 2023; Received in revised form 18 September 2023; Accepted 19 September 2023
Available online 19 September 2023
1050-4648/© 2023 The Authors. Published by Elsevier Ltd. This is an open access article under the CC BY license (http://creativecommons.org/licenses/by/4.0/).

1. Introduction

The antimicrobial peptide (AMP) NK-lysin, first identified in pig small intestine [1], exerts both antibacterial activity against Gram – and Gram + bacteria, and cytotoxic activity against tumoral cell lines. It was found in $CD8^+$, $CD2^+$ and $CD4^+$ cells, therefore considered an effector peptide of T- and NK-cells. The peptide showed a high positive net charge and it was included in the family of saposins-like proteins due to the presence of domains homologous to saposins A-D, the first representatives of this family to be characterized [2]. NK-lysin 3D structure was determined by NMR spectroscopy, becoming the first member of the saposins family for which a structure was known [3]. The 3D structure comprised of five amphipathic α-helices folded in a globular domain including three disulphide bonds that are conserved in most saposins. NK-lysin acted as a neutralizer agent against LPS in a specific mouse model for sepsis [4] and the peptide was able to bind to matrix-coated S-form of LPS from *Escherichia coli*, *Pseudomonas aeruginosa*, and *Streptococcus minnesota* [5]. The interaction of LPS with NK-lysin was determined in detail using NK-2, a derived peptide that corresponds to the highly charged core region of its precursor [6]. NK-2 was not only a potent antibacterial agent, but also a very efficient neutralizer of different LPS-chemotypes, and, in this way, it prevented the production of LPS-induced pro-inflammatory cytokines. Moreover, NK-2 was tested *in vitro* against the parasite *Trypanosoma cruzi* and it was able to rapidly permeabilize its plasma membrane as evidenced by inhibition of the mobility of trypomastigotes [7].

In the last years, NK-lysin homologues were identified in different fish species and their functional activity has been deeply investigated considering the intriguing results obtained for mammalian counterparts. The first NK-lysin fish sequences were found in channel catfish [8] and Japanese flounder [9]. A peptide derived from the latter, homologous to pig NK-2, exerted antibacterial activity against both Gram + and Gram – bacteria without showing any hemolytic activity. Most of the peptides derived from NK-lysin fish sequences later characterized in tongue sole [10], large yellow croaker [11], mudskipper [12], golden pompano [13] and black rockfish [14] displayed antibacterial activity. Some NK-lysin-derived peptides also provided *in vivo* protection against bacterial or virus infection, like those from tilapia infected with *Streptococcus agalactiae* [15], striped catfish and crucian carp with *Aeromonas hydrophila* [16,17] and European sea bass with nodavirus [18]. Moreover, NK-lysin peptides from turbot [19] and gibel carp [20] inhibited the proliferation of spring viraemia of carp virus (SVCV) in epithelioma papulosum cyprinid (EPC) cells. Finally, turbot NK-lysin provided protection against a protozoan ciliate (*Philasterides dicentrarchi*) probably via membrane disruption [21]. In a recent paper, NK-lysin was found to be expressed in turbot nucleated red blood cells and possibly involved in antiviral immunity through the autophagic process [22].

Our work is focused on two peptides derived from a NK-lysin homologue identified in the red-blooded Antarctic fish *Trematomus bernacchii*. We previously investigated the biological activity of another antimicrobial peptide, the trematocine, from the same species [23]. Marine animals from the Antarctic continent have evolved peculiar adaptations to live in an extreme environment and, therefore, they are intensively studied as a source of new bioactive molecules. The two peptides were analysed for their antibacterial activity against strains from clinical isolates and for their safety towards healthy mammalian cells. Moreover, we studied their anticancer activity against a mouse melanoma cell line exploring in detail the death process triggered by the peptides. Finally, we performed all-atom MD simulation to investigate the effects of the mutation on the structure of two NK-lysin peptides.

2. Materials and methods

2.1. Identification and structural characterization of the NK-lysin sequence

The nucleotide sequence of a putative NK-lysin was identified from the head kidney transcriptome of *T. bernacchii* [24]. In detail, the *Dicentrarchus labrax* NK-lysin precursor protein sequence (accession ID: ASD56696.1) was used as a query for a tBLASTn search performed setting an e-value threshold of 1×10^{-10}. Adult specimens of *T. bernacchii* were collected during the 37th Italian National Research Project in Antarctica (PNRA) at the Italian Antarctic Base, Terra Nova Bay, Ross Sea (Mario Zucchelli Station). After collection, 3 fishes were placed in tanks with running seawater. Muscle, brain, liver, gut, head kidney, spleen and gills were sampled and homogenized by teasing on a 100 μm cell strainer; the obtained cells were placed in vials containing Tripure (Roche, Basel, Switzerland) for total RNA extraction. Total RNA was resuspended in DEPC-treated water and quantified. cDNA was obtained using BioScript MMLV RNAse H minus (Bioline). The NK-lysin sequence was confirmed by PCR cloning of the entire coding region (data not shown) from gills cDNA. The signal peptide was identified using SignalP 6.0 [25] and a multiple sequence alignment of NK-lysins from fish species was carried out with CLUSTAL omega. The NK-lysin amino acid sequences were compared using the Pairwise Sequence Alignment Tool from EMBL-EBI. To pinpoint possible molecular signatures of cold adaptation, all non-synonymous mutations shared by >80% of the NK-lysin sequences from Cryonotothenioidea, but only observed in <40% of the other perciform species, were marked for further inspection. Their presence or absence in the two non-Antarctic notothenioids *Cottoperca gobio* and *Eleginops maclovinus* was used to discriminate between shared ancestral cold-independent polymorphisms and probable cold adaptation signatures. The 3D structure of *T. bernacchi* NK-lysin was predicted with AlphaFold 2 within the ColabFold v1.5.2 environment [26], using default settings.

2.2. Basal expression of NK-lysin

The basal expression of NK-lysin from *T. bernacchii* was determined with an Mx3000P real-time PCR system (Stratagene, San Diego, CA, USA) equipped with version 4.1 software and using the Brilliant SYBR Green Q-PCR Master Mix (Agilent Technologies, Santa Clara, CA, USA), following the manufacturer's instructions, with ROX as an internal passive reference dye. The organs and tissues from the three collected fishes were analysed. The reaction was performed using primers for the amplification of the product from NK-lysin and 18 S ribosomal RNA, used as a house-keeping gene (see Table I). The PCR conditions were: 95 °C for 10 min, followed by 35 cycles of 95 °C for 45 s, 52 °C for 45 s, and 72 °C for 45 s. Triplicate reactions were performed for each template cDNA. A relative quantification was performed using the Pfaffl's efficiency-calibrated method [27], comparing the levels of the target transcript (NK-lysin) to a reference transcript (calibrator, the tissue with the lowest NK-lysin expression), in this case, the muscle.

2.3. Peptides

The peptides (NKL-WT: KLKSKLMVVCNKIGLLKSLCRKFVKSH, and

Table 1
Primers used for expression analysis.

Gene	Primers sequence (5' – 3')(Forward, FW, Reverse, RV)	Accession number
NK-lysin	GGTGAAGAAAACGGTCGGACG (FW) GTGCAACAACTCCTTTGGCTTG (RV)	OM141133
18S ribosomal RNA	CCAACGAGCTGCTGACC (FW) CCGTTACCCGTGGTCC (RV)	AY831388

NKL-MUT: KLKSKLMVVANKIGLLKSLARKFVKSH, 98% purity) were purchased from GenicBio Limited (Shangi, China). Peptide concentration was determined for each sample preparation by UV light absorption.

2.4. Outer membrane permeability essay

The fluorescent probe 1-aminonaphtalene-8-sulfonic acid (ANS) uptake was used for cell permeabilization studies. Specifically, the Antarctic marine psychrotolerant bacterium *Psychrobacter* sp. TAD 1, *Escherichia coli* ATCC 25922, and *Bacillus cereus* ATCC 10876 were grown in the Luria Bertani (LB) medium, at 18 °C, 37 °C and 37 °C, respectively. Subsequently, three different cell suspensions were centrifuged at 3000 g, washed, using saline phosphate buffer (PBS), and resuspended in the analysis buffer (PBS) to achieve an OD_{600} of 0.6. Increasing amounts of peptide (ranging from 0 to 30 μM) were added to 700 mL of cell suspension in presence of 25 μM of ANS. Fluorescence spectra were recorded from 400 nm to 600 nm, at the PerkinElmer fluorometer LS 55 in steady-state at room temperature, using an excitation wavelength of 360 nm and excitation/emission band-pass of 5 nm. The disruption of cell membrane integrity was quantified by the increase in the intensity of fluorescence as per Olivieri et al. [28]:

$$\%\ \text{Uptake ANS} = (\text{F-F}_o)\text{x}100/\text{F}$$

where F is the fluorescence of ANS observed at a given peptide concentration and F_o is the fluorescence of ANS in the absence of peptides.

2.5. Antibacterial activity of peptides

2.5.1. Bacterial isolates

Several Gram - and Gram + bacteria collected at the Microbiology Institute of "IRCCS Fondazione Policlinico Universitario Agostino Gemelli" were tested. The strains (*Streptococcus pyogenes*, *Enterococcus faecalis*, *Staphylococcus capitis*, *Enterococcus faecium*, *Bacillus cereus*, *Escherichia coli*, *Acinetobacter baumannii* and *Klebsiella pneumoniae)* were isolated from blood cultures and cultivated in Mueller Hinton Agar (Oxoid, Basingstoke, UK) at 37 °C for 24 h prior to use in antibacterial assays.

2.5.2. Determination of the Minimum Inhibitory Concentration (MIC) of the AMPs

The *Minimum Inhibitory Concentration* (MIC) of NKL-WT and NKL-MUT AMPs towards the clinical isolates were determined *in vitro* by a microbroth dilution test in accordance with the European Committee on Antimicrobial Susceptibility Testing (EUCAST) guidelines [29]. MIC was defined as the lowest concentration of peptide at which no bacterial growth is observed compared with the growth of positive control. The microbroth dilution assays were performed in 96 well-plates and the peptides were used at a concentration ranging between 256 and 0.25 μg/mL. Bacterial suspensions in Mueller Hinton Broth (Oxoid, Basingstoke, UK) were used at a concentration to 10^5 cells/mL (1:100 of 0.5 McFarland). Subsequently, 50 μL of the microbial suspensions were added to each well containing the peptides at different scalar dilutions. The MIC values were visually determined, after 24 h of incubation at 37 °C.

2.5.3. Determination of the Minimum Bactericidal Concentration (MBC) of the AMPs

To evaluate the *Minimum Bactericidal Concentrations* (MBC), subcultures were obtained by pipetting 10 μL of each well content on Muller Hinton Agar (MHA) (Oxoid, Basingstoke, UK). MBC was defined as the lowest peptide concentration corresponding to death of 99.9% or more of the initial inoculum. Each test was performed in triplicate and both negative (i.e. medium only) and positive (i.e. growth control of untreated microorganisms) controls were included.

2.6. Hemolytic activity

The hemolytic assay was performed on rabbit erythrocytes (Rockland) maintained in Alsever's solution (Innovative Research). Briefly, after the removal of Alsever's solution, the erythrocytes were resuspended in PBS and counted using a hemocytometer. A suspension of 5×10^6 red blood cells was incubated with five dilutions (from 5 μM to 80 μM) of NKL-WT and NKL-MUT peptides in a 96-well microplate. As a negative control, erythrocytes were incubated with an equivalent amount of water (peptide solvent), while as a positive control, erythrocytes were added to Triton 1% v/v. The plate was incubated at 37 °C for 2 h and subsequently centrifuged at 1200 rpm × 3 min to separate the pellet from the supernatant. The absorbance of the supernatant was measured at 492 nm (Epoch 2, BioTek). Each data point was assayed in triplicate. The relative OD compared to the positive control defined the percentage of hemolysis.

2.7. Cytotoxicity assay against human and murine cell lines

The cytotoxicity of the NKL-WT and NKL-MUT peptides was tested on both primary human fibroblast cell line (FB789) and mouse melanoma cell line (B16–F10) grown respectively, in Dulbecco's Modified Eagle Medium (DMEM) and Iscove's Modified Dulbecco's Medium, containing 10% fetal calf serum (FCS) and antibiotics (penicillin–streptomycin, Gibco) at 37 °C in a humidified 5% CO_2 atmosphere. Cells were seeded on 96-well microplates at a density of 5×10^3 cells per well in 100 μL of the medium overnight. Then, five dilutions of each peptide (from 5 μM to 80 μM) were added to the cells and maintained for 12 h and 24 h. As a negative control, cells were grown in normal medium plus an equivalent amount of water (peptide solvent), while, as a positive control, cells were added to NaN_3 0.5% v/v. The cytotoxicity was determined by measuring the intracellular adenosine triphosphate (ATP) levels using the luciferase-based ATPlite assay (PerkinElmer, Waltham, MA, USA), according to the manufacturer's instructions. After 12 h and 24 h, the cells were lysed, and the lysates were transferred into opaque well plates (OptiPlate-96, PerkinElmer). The amount of emitted light, linearly correlated with the ATP concentration, was measured with a microplate luminometer (Victor II PerkinElmer) for 10 min in the dark. Six replicates per each dilution were performed. Cell viability values were expressed as the mean +SD and calculated as the percent values of the treated samples with respect to negative control.

2.8. Cytofluorimetric determination of apoptosis and necrosis

Primary human fibroblast (FB789) and mouse melanoma (B16–F10) cell lines were seeded in 6-well plates at a density of 5×10^5 cells per well. Then, cells were treated with two higher dilutions of NKL-WT and NKL-MUT peptides (40 μM and 80 μM) for 24 h. As a negative control, cells were grown in normal medium plus water (peptide solvent), while, as a positive control, 12 μg/mL and 8 μg/mL of puromycin were added to B16–F10 and FB789, respectively. After the treatment, cells were trypsinized, washed twice with ice-cold PBS and incubated in 100 μL of 1x Annexin V-binding buffer containing 5 μL Annexin V-FITC (Life Technologies) for 15 min at room temperature in the dark. Afterwards, cells were washed with ice-cold PBS and were added to 100 μL of 1x Annexin V-binding buffer plus propidium iodide (1 μg/mL, Life Technologies) and immediately analysed by flow cytometry (BD Accuri™ C6 Plus Flow Cytometer, BDBiosciences).

2.9. Tunel assay

Terminal Deoxynucleotidyl-Transferase mediated dUTP Nick End Labeling (TUNEL) assay was performed using DeadEnd™ Fluorometric

TUNEL System (Promega, Madison, WI, U.S.A.). Briefly, 6×10^4 mouse melanoma (B16–F10) cells were seeded on sterile glass coverslips inserted in a 24-well cell culture plate for 24 h at 37 °C. Then, cells were treated with the highest concentration (80 μM) of NKL-WT or NKL-MUT peptide for 6 h. As a negative control, cells were grown in normal medium plus water (peptide solvent). At the end of the treatment, cells were fixed in 4% paraformaldehyde at 4 °C and permeabilized with 0.2% Triton X-100. After that, cells were exposed to the equilibration buffer (Promega) for 10 min and, subsequently, incubated with the rTdT incubation buffer (Promega) at 37 °C for 1 h in the dark to allow the tailing of green fluorescent nucleotides to 3 –OH DNA ends. The reaction was stopped by adding the 2X SSC buffer (Promega) to the cells. Finally, cells were washed twice with PBS and coverslips were mounted onto microscope slides with Fluoroshield mounting medium plus DAPI (Sigma-Aldrich). Images were captured in bright-field using two channel fluorescence (360 nm/460 nm; 488 nm/509 nm) with a a Leica microscope LMD6 equipped with the software LAS-X (Leica).

2.10. Scanning electron microscopy

2.10.1. Bacterial strains

Mid-logarithmic phase *Enterococcus faecalis* (5×10^7 CFU/mL) and *Acinetobacter baumannii* (5×10^7 CFU/mL) were treated at MBC respectively with NKL-WT (16 μg/mL, 5 μM) and NKL-MUT (32 μg/mL, 10 μM) peptides for 24 h. The growth medium without peptides was used as negative control. After incubation, the bacteria were harvested by centrifugation at 14.000 rpm for 20 min, washed 3 times with PBS and fixed with 2% paraformaldehyde and 2.5% glutaraldehyde in 0.1 M cacodylate buffer (Electron Microscopy Science) at pH 7.2 for 3 h at 4 °C. The specimens were then washed four times with a cacodylate buffer and then post-fixed with 1% osmium tetroxide (Electron Microscopy Science) in 0.1 M cacodylate buffer at pH 7.2 for 1 h at 4 °C. After washing in distilled water, the samples were dehydrated for 10 min in progressively increasing concentration of ethanol solutions (10% 30%, 50%, 70% and 90%), and for 15 min in 100% ethanol. Then, the samples were dried using the method of liquid CO_2 in a Critical Point Dryer (Balzers Union CPD 020), coated with gold in a Sputter Coater (Balzer Union MD 010) and examined using a Jeol JSM 6010 LA (Tokyo, Japan).

2.10.2. Mammalian cell lines

FB789 and B16F10 cells were seeded on sterile glass coverslips inserted in 24-well cell culture plates at a density of 6×10^4 cells per well. The cells were cultured for 24 h at 37 °C in a humidified incubator with 5% CO_2 atmosphere and then exposed to the two highest concentrations of NKL-WT and NKL-MUT peptides (40 μM and 80 μM) for 24 h. Negative controls were carried out by adding fresh medium. At the end of the treatments, the cells were washed twice, fixed, dehydrated and coated with gold as described for bacteria (*2.10.1*). Then, the samples were examined using a Jeol JSM 6010 LA (Tokyo, Japan).

2.11. Transmission electron microscopy

Enterococcus faecalis and *Acinetobacter baumannii* were treated at MBC, respectively with NKL-WT (16 μg/mL, 5 μM) and NKL-MUT (32 μg/mL, 10 μM) peptides for 24 h, then fixed as described for SEM analysis (*2.10.1*). After dehydration in ethanol solutions, the specimens were transferred to mixtures of acrylic resin LRWhite (London Resin White) and ethanol (v:v = 1:2, v:v = 1:1 and v:v = 2:1) for 1 h each step and then to pure acrylic resin overnight. The embedding was carried out using hermetic gelatin capsules. The samples were left to polymerize for 36 h at 50 °C. Ultrathin sections, 60–80 nm thick, were then obtained using an ultramicrotome, stained with uranyl acetate and lead citrate, and observed using a Jeol 1200 EX II TEM equipped with an Olympus SIS Veleta CCD camera and the iTEM software for image acquisition and processing.

2.12. Molecular dynamics simulations

The initial structure of NKL-WT and NKL-MUT were obtained by the I-Tasser web server [30]. Each peptide was solvated in a cubic box of $5 \times 5 \times 5$ nm^3 and 8 chloride ions were added to neutralize the charged residues of peptide.

All the molecular dynamics simulations were performed using GROMACS [31]. The bonding and non-bonding interaction were modelled by using CHARMM36 force field [32]. Water was modelled with the TIP3P model [33]. Non-bonding interactions were calculated using a cut-off of 1.2 nm. The particle mesh Ewald (PME) method [34] was applied to the long-range electrostatic interactions. The algorithms P-LINCS [35] and SETTLE [36] were used to constrain the bonds of peptides and water molecules respectively. The simulated systems were energy minimised and equilibrated in NPT ensemble at 310 K and 1 bar by using the velocity-rescale thermostat [37] and Berendsen barostat [38]. The pressure in the production phase was controlled by using the Parrinello-Rahman barostat [39]. Each system was simulated for 500 ns at 310 K and the initial 300 ns of the production phase were excluded for the analysis. The trajectories obtained by MD simulation were analysed with the GROMACS analysis tools, VMD 1.9.3 [40]. The secondary structure of peptides was calculated with the gmx do_dssp tool of GROMACS using the program DSSP [41].

2.13. Statistical analysis

Data analysis was conducted in the RStudio environment, R version 4.3.0, using the *readxl* package for raw data input, the *tidyverse* package for data manipulation and transformation, the *rstatix* package for conducting statistical tests, and the *ggpubr* and *RColorBrewer* packages for annotated data visualization in the form of boxplots and overlaid individual data points.

Normality and homoscedasticity assumptions for conducting parametric analysis were verified statistically by means of the Shapiro and Levene tests, and visually through the inspection of residuals in a normal quantile (QQ) plot. Non-parametric tests were conducted in case raw or log-transformed data did not satisfy the above-mentioned assumptions.

Raw hemolysis data per peptide concentration and type was subtracted from the negative control treatment absorbance and normalized to positive controls. Scaled data (i.e. 0 to 1) was analysed for within-effect (i.e. hemolytic rate ~ concentration, grouped by peptide type) using a Welch One-Way ANOVA followed by a *t*-test for pairwise comparisons setting the positive control as reference group.

Raw ATPlite data per cell line per incubation time per peptide type were first normalized to negative control. Scaled data (i.e. 0 to 1) was employed in statistical tests: the effect of the wild type peptide on B16F10 ATP levels was modelled with a Welch One-Way ANOVA followed by a *t*-test for pairwise comparisons setting NC as reference group; the effect of the mutant peptide on B16F10 ATP levels, as well as those of both peptide types on FB789 ATP levels, were modelled by Kruskal-Wallis rank sum tests followed by Wilcoxon tests for pairwise comparisons setting NC as reference group.

qPCR data, i.e. $\log_2$ fold changes, was modelled using tissue as predictor variable. The *p*-value of the model was adjusted by Holm correction and ges (generalized eta squared) was calculated as effect size. Pairwise differences among factor levels were calculated by the Tukey Honest Significant Differences test.

3. Results

3.1. NK-lysin sequence characterization and peptide selection

The nucleotide sequence of the NK-lysin mined from the head kidney transcriptome of *T. bernacchii* was confirmed by cloning its entire coding region from gills cDNA (data not shown) and deposited in GenBank under the accession ID OM141133.1. The translated amino acid

sequence contained 158 amino acid residues with a 22 aa-long signal peptide and six cysteine residues in the Saposin-like domain (amino acid positions 46–124), that corresponds to the putative mature region of the AMP (see Fig. 1, Panel A). A multiple alignment was assembled with NK-lysin sequences from other teleosts (Fig. 1, Panel A) to evidence the conserved amino acids. The Saposin-like domain showed high percentage of identity (as an example, 78.2% with both *Larimichthys crocea* and *Sparus aurata*) with the full conservation of cysteine residues among all mature peptides. A comparative analysis between the mature peptide sequences NK-lysin orthologs from Cryonotothenioidea, the non-Antarctic notothenioid species *Cottoperca gobio* and *Eleginops maclovinus*, and other perciform lineages highlighted the presence of two sites characterized by the presence of cryonotothenioid-specific non-synonymous mutations, which may point to cold adaptation signatures (Table S1).

Although the homology between NK-lysin peptides from *T. bernacchii* and *Sus scrofa* (accession number Q29075) was quite low (27.8% identity and 51.9% similarity), AlphaFold2 prediction confirmed the high conservation of the 3D structure (Fig. S1). They are both 78 amino acids long and the cysteine residues are maintained in the same positions, suggesting that three disulfide bridges could also be formed in the fish sequence between the same known pairs for the mammalian sequence (Cys4-Cys76, Cys7-Cys70 and Cys35-Cys45). A 27 aa peptide within the *T. bernacchii* NK-lysin sequence, partly corresponding to the potent antibiotic peptide NK-2 found in human NK-lysin (accession number CAA38035) (see Fig. 1, Panel A) [6], was selected to investigate its antibacterial and anticancer activities (named NKL-WT). Finally, taking into consideration the presence of two cysteine residues, we synthesized this peptide with a formed disulfide bond (to avoid the production of dimers and multimers) and a mutant in which two alanine substitute the two cysteine residues (see Fig. 1, Panel B, named NKL-MUT) to investigate the functional importance of this specific bond.

3.2. Basal expression of NK-lysin

Basal mRNA expression of NK-lysin was investigated in different organs and tissues of unstimulated and healthy *T. bernacchii* specimens by real-time PCR (Fig. 2). The transcript had the highest abundances in

A)

```
                                                          <Saposin-like
Cypcar      MLRRIVLITLL--ISSVCALHLEMRKEESTGNEFEESSGEIETEQLPGKCWACKWVMRKL    58
Orenil      MEMPSLIFPCLVATFSVRAVHGRTLEVSIDDEEDVDMEVLM---GLPGKCWACKWILNKV    57
Larcro      MNSSSVLFVCILGACSVWTVHGRNLKVNDDDQEGAELDISVEARKLPGLCWVCKWSLNKV    60
Treber      MDTSSILIVCILVTCSVWTIHGRSIKVNIDDQEPGEMEISVEAGKLPGVCWACKWALNKV    60
Diclab      METSSVLLVCILVTCSVWTVHGRNIKVKTDDQ--VDVQISVEAGKLPGLCWACKWALKKV    58
Spaaur      MEQSSVLLVCILVTCCVWTVHGRTLQINTDDQEPVDIEISGEAGKIPGICWACKWALNKV    60
Scomax      METSSVLLVCILVTCSVWTVHGRSLEINIDDQEQVDVAISVEAGKLPGKCWACKWALNKV    60
Paroli      MGTSSILLLCILVTCSVWTVKGRCFEIEIDDQEPVDVEPSVEAGKLPGKCWACKWALNKV    60
            *    :::  :    .* ::: .  : .  .:   :         :** **.*** :.*:
                  domain
Cypcar      KKQISNGATPDDIKTKLGMVCDEIGFLKSICRKLVNQYTDTLVEELSTTDDARTICANIG    118
Orenil      KKLAGPNPTAESLKSKLLSVCDGIGLLKSLCRKFVKAHLGELIEELTTTDGVRTICVNMG    117
Larcro      KKLLGRNTTAESVKEKLMRVCNEIGLLKSLCKKFVKGHLGELIEELTTSDDVRTICVNLK    120
Treber      KKTVGRNATAEKLKSKLMVVCNKIGLLKSLCRKFVKSHLPVLIEELTTTDDVRTICVNTK    120
Diclab      KKVMGPNATAENMTPKLLAVCDQIGLLKSLCRKFVKKHLGELIEELTTTDDVKTICVNTG    118
Spaaur      KKVIGPNATTESVTTKLNSVCNEIGLLKALCRKFVKAHLGELIEELTTTDDVRTICVNTG    120
Scomax      KKVMGPNVTSEGVKSKLNIVCNEIGLLKSLCRKFVNSHIWELVEELSTTDDVRTICVNTG    120
Paroli      KRIIGRNATAESMKSKLNVICNEIGLLKSLCRKFVKTHLGELIEELTTTDDVRTICVNTG    120
            *:  . . * : :. **  :*: **:**::*:*:*: :   *:***:*:*..:***.*

               >
Cypcar      VCKK---------------------------------- 122
Orenil      ACKSKELE-LLFYAENGGPLIDVKELD------------ 143
Larcro      ACKPKELSELDFESD-EDAHTEMNDLLFE---------- 148
Treber      ACKPKELLHQVYQSDDGGVQIQMNEYPEGRIAWMNKTM 158
Diclab      ACKPKEMLDLLFYSSDEDSQIEMNEYAWG---------- 147
Spaaur      ACKPKEWVNLLFYRSDVDAKFEMIDYP------------ 147
Scomax      ACEPKQLSHLLFYPKQEESQTEIIEYS------------ 147
Paroli      ACQPKEVAHLLFRPKHDESQTEIIEYP------------ 147
            .*:
```

B)

```
NKL-WT   KLKSKLMVVCNKIGLLKSLCRKFVKSH   27

NKL-MUT  KLKSKLMVVANKIGLLKSLARKFVKSH   27
```

Fig. 1. Panel A) Multiple alignment of the predicted NK-lysin amino acid sequence from *Trematomus bernacchii* with other known homologues from Teleost fish [accession numbers: *Cyprinus carpio* (Cypcar) KX034213.1; *Oreochromis niloticus* (Orenil) MF678822.1; *Larimichthys crocea* (Larcro) KJ865299.1; *Trematomus bernacchii* (Treber) OM141133; *Dicentrarchus labrax* (Diclab) KY801205.1; *Sparus aurata* (Spaaur) MN240490.1; *Scophthalmus maximus* (Scomax) KU705506.1; *Paralichthys olivaceus* (Paroli) AU260449.1. The conserved Saposin-like domain in all sequences is shown above the alignment. The identical amino acids are indicated with an "*" below the alignment, while "." and ":" show amino acids with conserved physical and/or chemical properties. The signal peptide for the *Trematomus bernacchii* NK-lysin sequence is evidenced in italics. The putative *Trematomus bernacchii* NK-lysin mature sequence is highlighted in red, the position of the six cysteine residues found inside the sequence is shown in bold and the selected peptide is both underlined and in bold. **Panel B)** An alignment of the 27 amino acids long selected NK-lysin peptide (wild-type-NKL, NKL-WT) from *Trematomus bernacchii* and the mutant (mutant-NKL, NKL-MUT) where the two cysteine residues have been substituted by alanine residues.

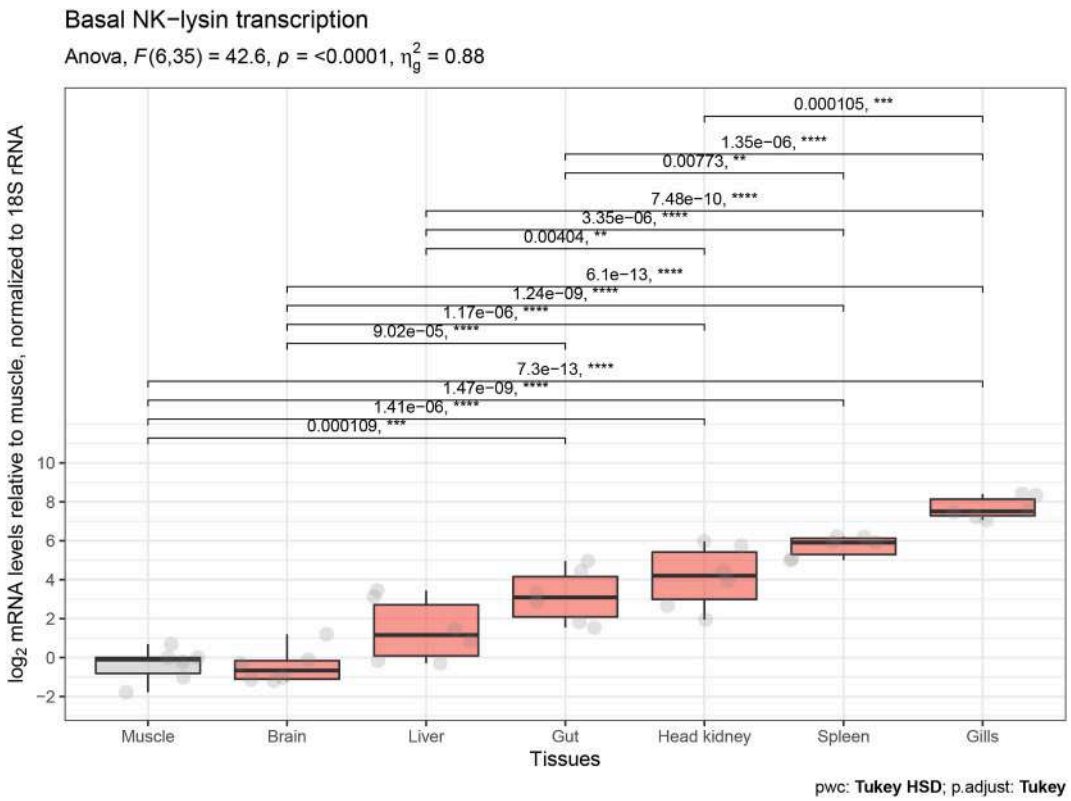

Fig. 2. NK-lysin basal expression in different tissues. NK-lysin mRNA levels were expressed as a ratio to 18S rRNA levels in the same samples after real-time PCR analysis using the tissue with the lowest expression (muscle) as the calibrator.

immune-relevant organs (i.e. gills, spleen, head kidney and gut in descending order), followed by liver and brain. A one-way ANOVA was conducted to identify the effect of tissues on NK-lysin transcription: a significant main effect of tissue was found on mRNA expression ($F_{(6,35)} = 42.60$, $p = 1.16 \times 10^{-14}$), with the predictor variable describing 88% of the model variance.

3.3. Outer membrane permeability assay

The capability of NKL-WT and NKL-MUT peptides to permeabilize the outer membrane of Gram-negative bacteria (*Escherichia coli* ATCC 25922 and Psychrobacter sp. TAD 1) and the plasmatic membrane of Gram-positive bacteria (*Bacillus cereus* ATCC 10876) was assessed by a membrane permeability assay using ANS as a fluorescent probe.

The fluorescence of ANS is relatively weak in aqueous solution and strong in a hydrophobic environment. In the presence of intact bacterial cells, ANS is not able to enter the wall cell, and the fluorescence is weak because of the high polarity of the medium. However, upon adding peptides capable of disrupting the cell membrane integrity, the ANS is incorporated into the lipid bilayer, and its fluorescence intensity increases drastically [42]. Fig. 3 A-B shows the percentage of ANS uptake along the increasing concentrations of tested peptides.

The NKL-WT peptide had a good ability to alter the plasmatic membrane of *Bacillus cereus* and the outer membrane of *Escherichia coli*, whereas the NKL-MUT peptide had a weaker effect. In fact, the ANS uptake at 5 μM NKL-WT is 73% for the Gram - and 91% for the Gram + bacteria, compared to 50% and 42%, respectively, for the NKL-MUT peptide at the same concentration. Both peptides showed the same effect on *Psychrobacter* sp. TAD 1.

3.4. Antibacterial activity of peptides

Table II shows the obtained MIC values for the two tested peptides. The NKL-WT displayed a MIC value of 16 μg/mL against different Gram - and Gram + bacteria. Specifically, the peptide induced a significant inhibition of bacterial growth versus *Streptococcus pyogenes*, *Enterococcus faecalis*, *Escherichia coli* and *Staphylococcus capitis*. On the contrary, MIC values ≥ 64 μg/mL were found against *Acinetobacter baumannii*, *Klebsiella pneumoniae*, *Enterococcus faecium* and *Bacillus cereus*, which were consequently less susceptible. The NKL-MUT peptide showed MIC values against *Acinetobacter baumannii* and *Klebsiella pneumoniae* of 8 and 32 μg/mL, respectively, and against *Escherichia coli* of 16 μg/mL, whereas it was ineffective against *Streptococcus pyogenes*, *Staphylococcus capitis*, *Enterococcus faecalis*, *Enterococcus faecium* and *Bacillus cereus*, with MIC values ≥ 64 μg/mL. With regards to MBC values, NKL-WT was active against *Enterococcus faecalis* (16 μg/mL) and NKL-MUT against *Acinetobacter baumannii* (32 μg/mL) (Table III).

3.5. Hemolysis

Hemolytic activity of wild type and mutant peptides was assessed at several concentrations against rabbit erythrocytes and normalized to a positive control treatment consisting of 1% Triton X-100 treated erythrocytes (Fig. 4). The hemolytic effect was found to follow a dose dependency pattern for the wild type peptide, with the two highest concentrations of 40 and 80 μM causing a hemolytic rate of 16.3% and 40.5%, respectively. On the other hand, the NKL-MUT peptide provoked extremely low and dose-independent hemolytic rates ranging from 0.9% at 5 μM to 2.6% at 80 μM. A significant effect of concentration was found for both the wild type ($F_{(5,\ 8.08)} = 213.54$, $p = 2.34 \times 10^{-8}$) and mutant ($F_{(5,\ 18.73)} = 486$, $p = 7.76 \times 10^{-19}$) peptides. The null hypothesis of hemolysis being equally induced by both peptide types at given concentrations was rejected for the three highest concentrations, i.e. 20 μM ($t_{(3.43)} = 6.08$, $p = 2.38 \times 10^{-2}$), 40 μM ($t_{(5.68)} = 19.34$, $p = 1.26 \times 10^{-5}$) and 80 μM ($t_{(3.06)} = 11.54$, $p = 6.4 \times 10^{-3}$).

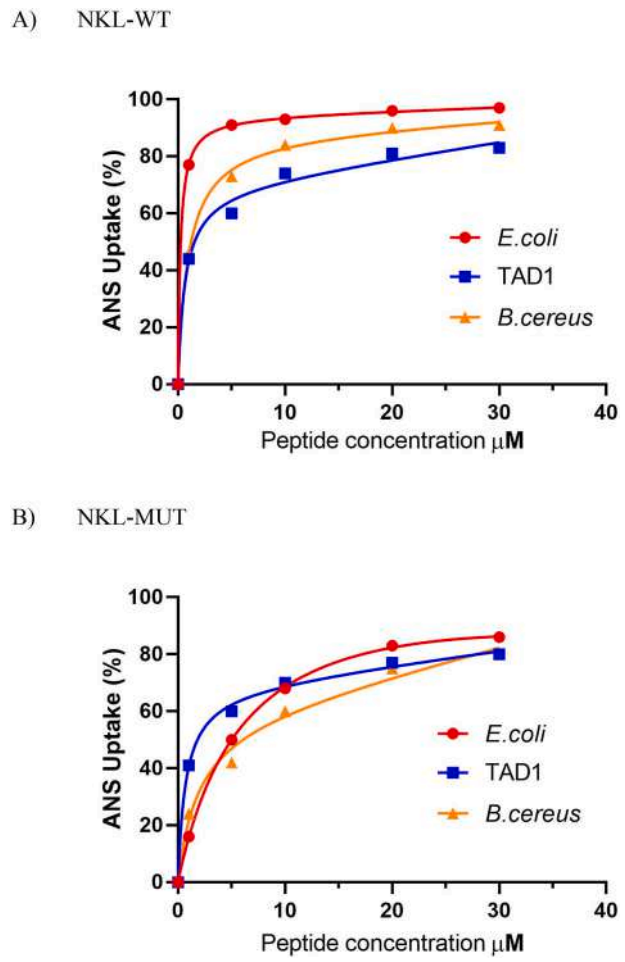

Fig. 3. Percentage of ANS uptake of *Bacillus cereus*, *Escherichia coli* and *Psychrobacter* sp. TAD 1 as a function of peptide NKL-WT (A) and NKL-MUT (B) concentration.

Table 2
MIC values (μg/mL) against different Gram - and Gram + isolates.

	MIC	
Microorganism	NKL-WT	NKL-MUT
Escherichia coli	16 μg/mL (5 μM)	16 μg/mL (5 μM)
Acinetobacter baumannii	64 μg/mL (20 μM)	8 μg/mL (3 μM)
Klebsiella pneumoniae	128 μg/mL (40 μM)	32 μg/mL (10 μM)
Streptococcus pyogenes	16 μg/mL (5 μM)	64 μg/mL (20 μM)
Enterococcus faecalis	16 μg/mL (5 μM)	128 μg/mL (40 μM)
Staphylococcus capitis	16 μg/mL (5 μM)	64 μg/mL (20 μM)
Enterococccus faecium	>64 μg/mL (>40 μM)	>64 μg/mL (>40 μM)
Bacillus cereus	>64 μg/mL (>40 μM)	>64 μg/mL (>40 μM)

Table 3
MBC values (μg/mL) against *E. faecalis* and *A. baumannii*.

	MBC	
Microorganism	NKL-WT	NKL-MUT
Enterococcus faecalis	16 μg/mL (5 μM)	128 μg/mL (40 μM)
Acinetobacter baumannii	64 μg/mL (20 μM)	32 μg/mL (10 μM)

3.6. Cell viability

ATP levels of B16F10 exposed to the NKL-WT peptide ranged between 0.01 and 1.26, normalized to negative controls, regardless of incubation time and peptide concentration. B16F10 ATP levels at 12 h and 24 h time points are depicted in Fig. 5 A: the Welch ANOVA tests returned a strong statistical significance of peptide concentration on ATP levels for both time points (12 h: $F_{(6,\ 26.6)} = 490.63$, $p = 5.72 \times 10^{-26}$; 24 h: $F_{(6,\ 30.23)} = 735.38$, $p = 4.80 \times 10^{-31}$). Pairwise comparisons against NC as a reference group returned statistically significant differences for the three highest peptide concentrations at 12 h, and for concentrations 5, 20, 40 and 80 μM at 24 h (Fig. 5 A).

ATP levels of B16F10 exposed to the NKL-MUT peptide ranged between 0.04 and 1.27, normalized to negative controls, regardless of incubation time and peptide concentration. B16F10 ATP levels at 12 h and 24 h time points are depicted in Fig. 5 B: the Kruskal-Wallis H tests showed a statistically significant difference in ATP levels among concentrations for both time points (12 h: $\chi^2_{(6)} = 109.52$, $p = 5.14 \times 10^{-21}$; 24 h: $\chi^2_{(6)} = 57.10$, $p = 1.74 \times 10^{-10}$). Pairwise comparisons against NC as a reference group returned statistically significant differences for all peptide concentrations at both time points, with a less steep decrease in ATP median levels than what was observed with the wild type peptide (Fig. 5B). The mutant peptide induced less severe ATP decreases at 40 and 80 μM than the wild type at either time points (Fig. 5C): at 12 h, 0.753 ± 0.254 and 0.34 ± 0.193 normalized ATP levels (mutant) were found instead of 0.023 ± 0.007 and 0.016 ± 0.002 (wild type), respectively; at 24 h, 0.851 ± 0.096 and 0.232 ± 0.075 (mutant) were measured compared to 0.019 ± 0.004 and 0.014 ± 0.002. The above descriptive statistics are expressed as mean ± standard deviation.

ATP levels measured on the FB789 cell line exposed to the NKL-WT peptide ranged between 0.03 and 1.72, normalized to negative controls, regardless of incubation time and peptide concentration. FB789 ATP levels at 12 h and 24 h time points are depicted in Fig. 6 A: the Kruskal-Wallis H tests returned a strong statistical significance of peptide concentration on ATP levels for both time points (12 h: $\chi^2_{(6)} = 63.33$, $p = 9.46 \times 10^{-12}$; 24 h: $\chi^2_{(6)} = 68.19$, $p = 1.92 \times 10^{-12}$). ATP decreased significantly compared to NC at 40 and 80 μM at both time points.

ATP levels of FB789 exposed to the NKL-MUT peptide ranged between 0.13 and 2.32, normalized to negative controls, regardless of incubation time and peptide concentration (Fig. 6B). The Kruskal-Wallis H tests returned statistically significant difference in ATP levels among concentrations for both time points (12 h: $\chi^2_{(6)} = 44.24$, $p = 6.60 \times 10^{-8}$; 24 h: $\chi^2_{(6)} = 62.05$, $p = 3.46 \times 10^{-11}$). A pattern of ATP increase was noted across concentrations, especially at 12 h, even though data at this time point were characterized by a greater dispersion than at 24 h. Overall, incubation of FB789 with the mutant peptide resulted in higher ATP levels than when exposed to the wild type, and did not result in any cytotoxicity, even at the two highest doses (Fig. 6C).

3.7. Evaluation of NKL-WT and NKL-MUT peptides induced-cell death

An apoptosis assay was performed using Annexin V/PI double staining to identify cell death mechanisms underlying NKL-WT and NKL-MUT peptides toxicity after 24 h treatment (Figs. 7 and 8). Peptides concentrations of 40 μM and 80 μM were chosen based on cytotoxicity data. B16F10 cell line treated with NKL-WT showed apoptotic rate percentages (early apoptosis + late apoptosis) of 35.7% (40 μM) and 78.7% (80 μM) with necrotic percentages of 3.1% and 16.8% respectively (Fig. 7). The treatment with NKL-MUT peptide induced higher death percentages: 56.3% of apoptotic rate and 38.7% of necrosis for the 40 μM concentration, and 86% of apoptosis and 11.3% of necrosis for the 80 μM treatment (Fig. 7). On the other hand, FB789 cells showed higher apoptotic rate when treated with NKL-WT at both concentrations: 14.3% (40 μM) and 94.6% (80 μM) with necrotic percentages of 5.7% and 4.2%, respectively (Fig. 8). The treatment with NKL-MUT peptide induced much lower apoptotic percentages similarly to the control group: 9.6% of apoptotic rate and 5.8% of necrosis for the 40 μM concentration, and 13.2% of apoptosis and 10.1% of necrosis for the 80 μM treatment (Fig. 8). The apoptotic effect of NKL peptides on B16F10 cells was confirmed by TUNEL assay (Fig. 9). The treatment with 80 μM NKL-

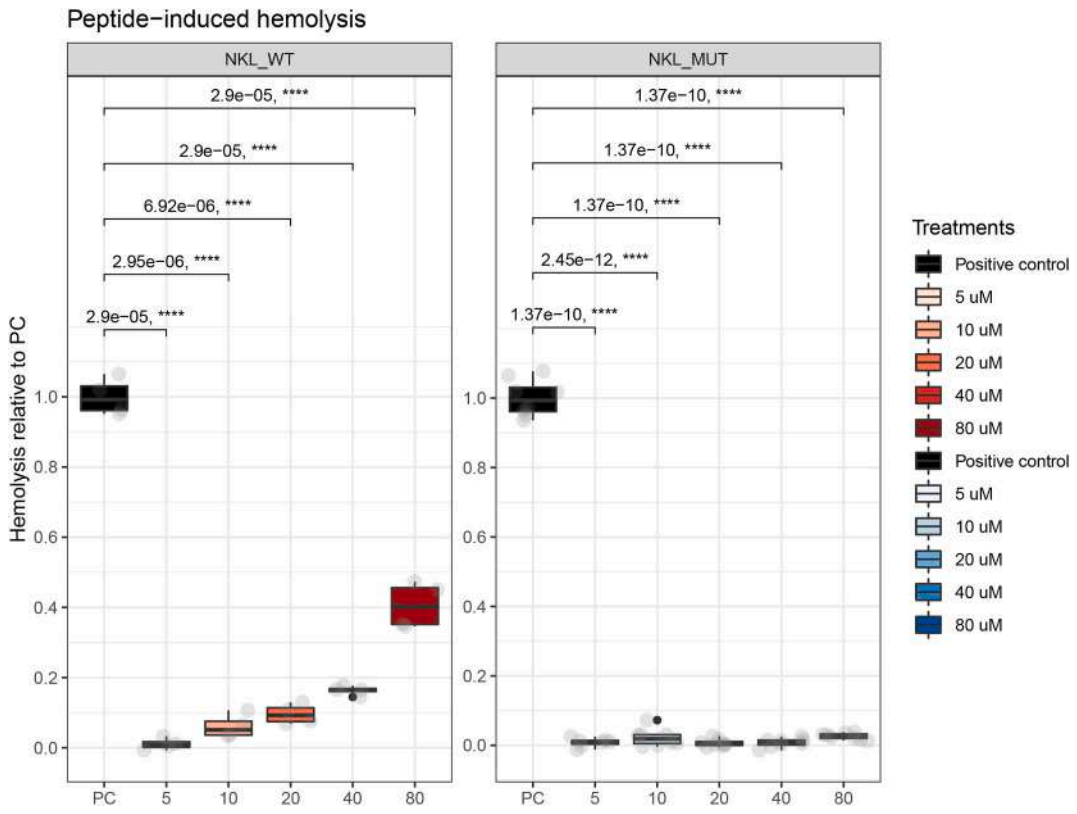

Fig. 4. Peptide-induced hemolytic activity detected in rabbit erythrocytes expressed as percentage relatively to positive control (i.e. erythrocytes incubated with Triton 1% v/v), per peptide type and concentration.

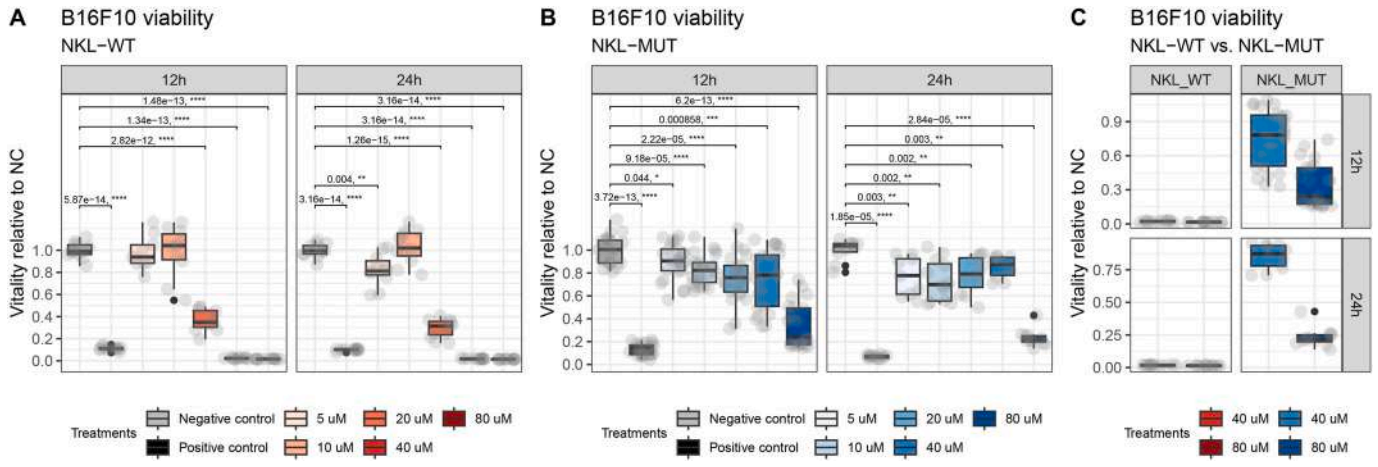

Fig. 5. B16F10 ATP levels as a proxy of viability, expressed relatively to negative controls, following a 12- and 24-h incubation with 5–80 μM of wild-type (A) or mutant (B) peptides. Concentrations are color-coded. C) Focus on viability detected following incubation with the two highest concentrations.

MUT peptide (Fig. 9A–C) enhanced nucleic DNA fragmentation compared to NKL-WT treatment (Fig. 9D–F) and negative control (Fig. 9G–I).

3.8. Evaluation of structural and morphological changes induced by NKL-WT and NKL-MUT peptides to Enterococcus faecalis and Acinetobacter baumannii

Scanning electron microscopy (SEM) and transmission electron microscopy (TEM) were used to examine the ultrastructural changes induced in *Enterococcus faecalis* and *Acinetobacter baumannii* (Figs. 10 and 11), selected by reference to the MBC values for NKL-WT and NKL-MUT peptides, respectively (Table 3).

3.8.1. Scanning electron microscopy

Untreated *E. faecalis* cells displayed round shape, smooth and intact surface (Fig. 10 A). The exposure to the established MBC for NKL-WT peptide (16 μg/mL, 5 μM) caused morphological changes, and lysed many *E. faecalis* cells (Fig. 10 B). Untreated *A. baumannii* cells exhibited rod shape and appeared undamaged (Fig. 10C). After incubation with NKL-MUT peptide (32 μg/ml, 10 μM) numerous lysed cells and cell debris were observed (Fig. 10 D).

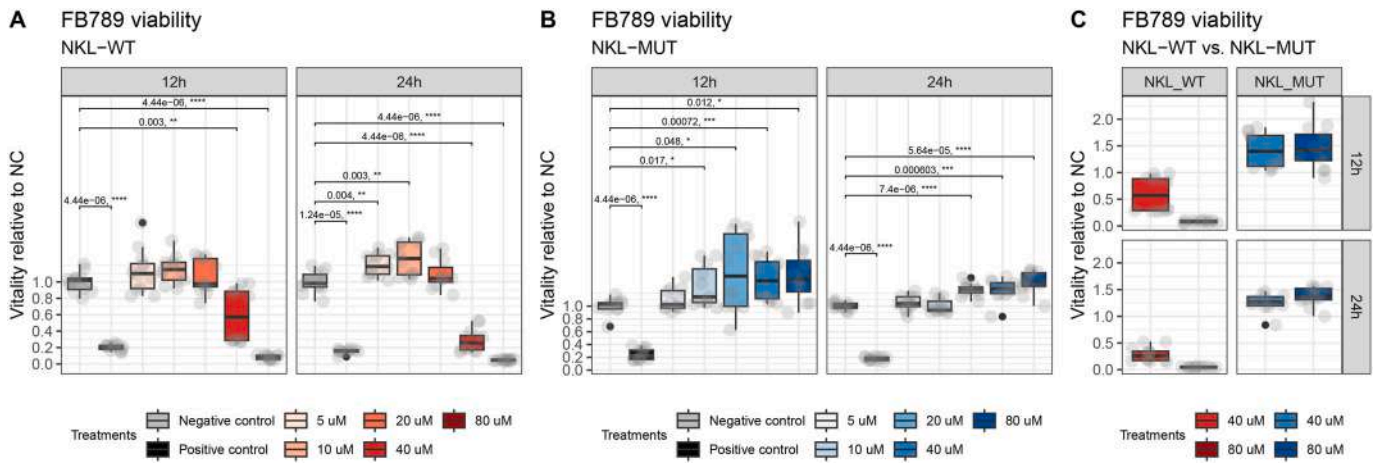

Fig. 6. FB789 ATP levels as a proxy of viability, expressed relatively to negative controls, following a 12- and 24-h incubation with 5–80 μM of wild-type (A) or mutant (B) peptides. Concentrations are color-coded. C) Focus on viability detected following incubation with the two highest concentrations.

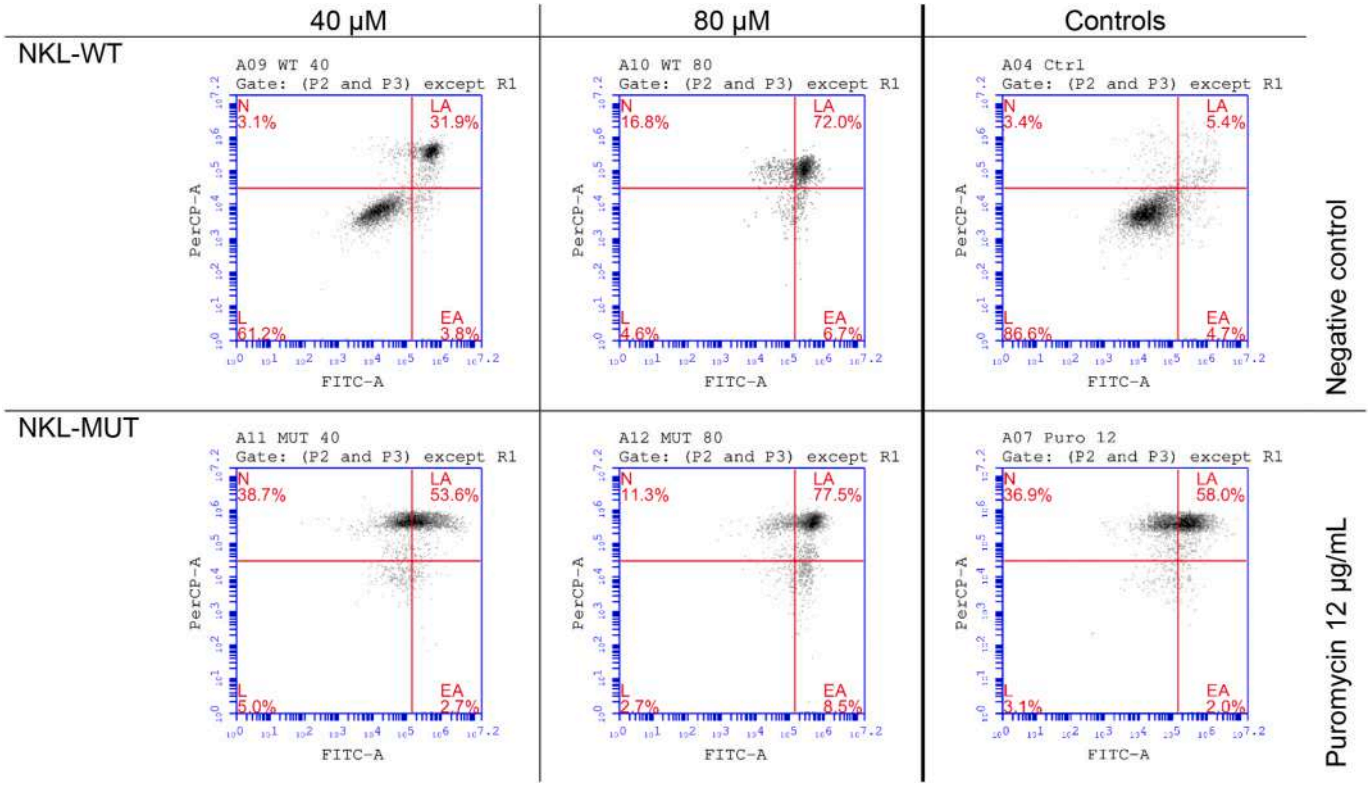

Fig. 7. Flow cytometric Annexin V/Propidium Iodide staining assay of B16F10 cells following a 24-h incubation with two concentrations of wild type and mutant NK-lysin. Percentages at each quadrant corner indicate positivity of viable (L), early/late apoptotic (EA/LA) or necrotic (N) cells. Propidium iodide and annexin V fluoresces read by PerCP (Peridinin-Chlorophyll-Protein) and FITC (Fluorescein isothiocyanate) fluorescence.

3.8.2. Transmission electron microscopy

TEM micrographs of *E. faecalis* in standard medium showed round proliferating cells with intact walls and well-defined membranes. The intracellular DNA region displayed heterogeneous electron density (Fig. 11 A). After incubation with NKL-WT peptide (Fig. 11 B), it was possible to observe the appearance of many vacuoles. The treatment induced loss of intracellular content, with genetic material spread across the cytoplasm. Moreover, the bacterial cell wall was undistinguished and membrane disruption was observed. A similar trend was found for NKL-MUT, which targets *A. baumannii* cells. Such exposure induced outer and inner membranes disruption, loss of cellular components, appearance of vacuoles and translucent zones (Fig. 11 D). Untreated *A. baumannii* cells were intact and exhibited well-defined membranes. The DNA region displayed heterogeneous electron density (Fig. 11C).

3.9. Assessment of morphological changes induced by NKL-WT and NKL-MUT peptides on FB789 and B16F10 cell lines

SEM analysis was carried out to assess peptide-induced effects on human fibroblasts (FB7689) and murine melanoma (B16F10) cell morphology. FB7689 and B16F10 cells were exposed to the two highest concentrations of NKL-WT and NKL-MUT peptides (40 μM and 80 μM), selected on the basis of cytotoxicity data, and compared to control cells (Figs. 12 and 13). FB789 untreated cells (negative control) appeared as

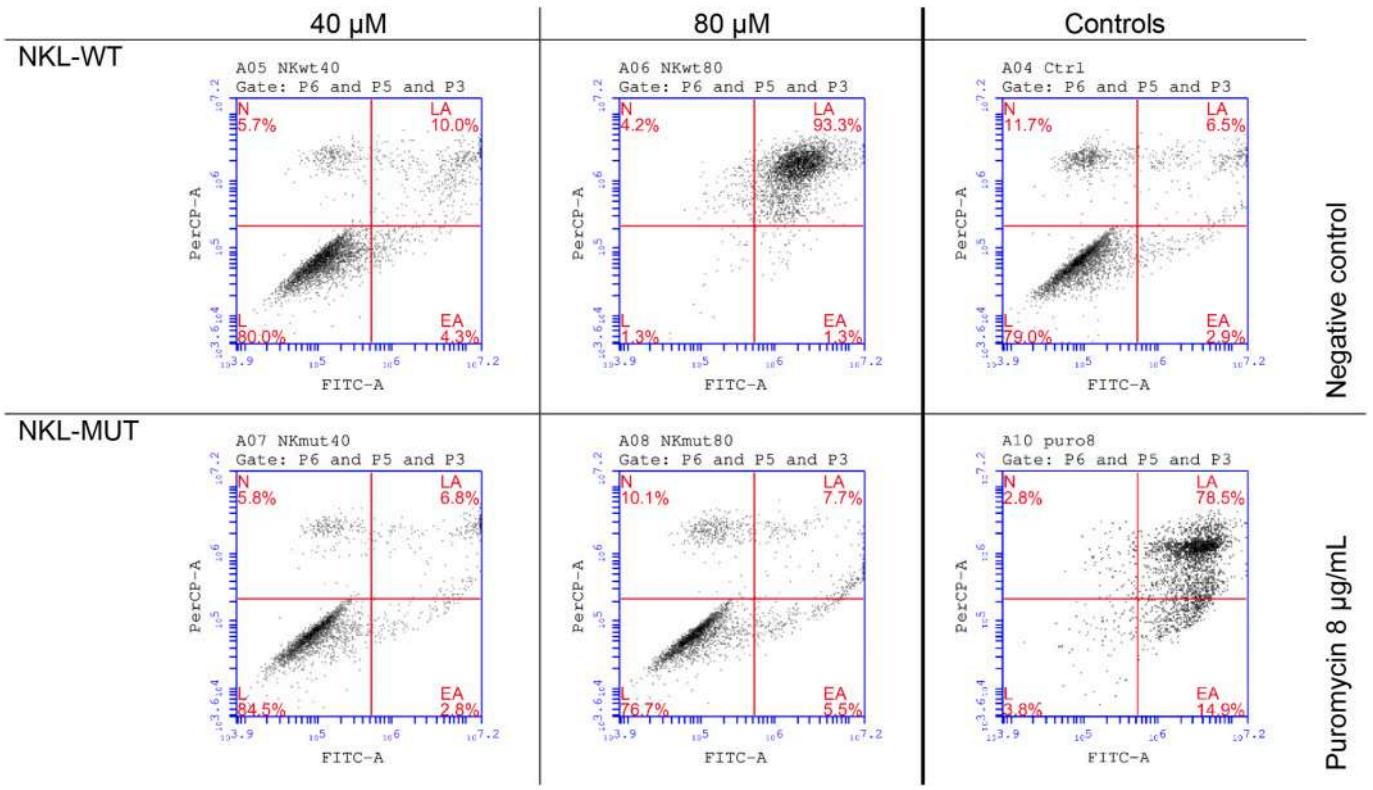

Fig. 8. Flow cytometric Annexin V/Propidium Iodide staining assay of FB789 cells following a 24-h incubation with two concentrations of wild type and mutant NK-lysin. Percentages at each quadrant corner indicate positivity of viable (L), early/late apoptotic (EA/LA) or necrotic (N) cells. Propidium iodide and annexin V fluoresces read by PerCP (Peridinin-Chlorophyll-Protein) and FITC (Fluorescein isothiocyanate) fluorescence.

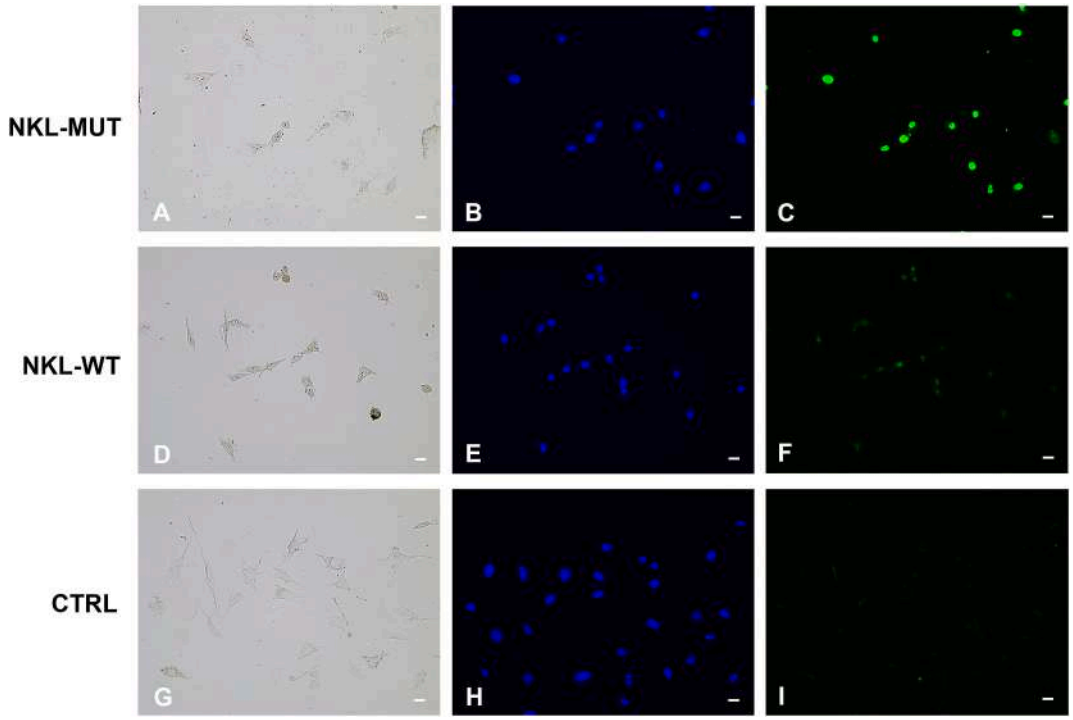

Fig. 9. TUNEL assay of B16F10 cells treated with 80 µM wild type and mutant peptides for 24 h. Representative images of bright field, Dapi staining of nuclei (blu) and Tunel (green) of NK-MUT peptide (A–C), NK-WT peptide (D–F) and control (G–I). Scale bar: 20 µm.

plump spindle shaped cells with flat nucleus, cytoplasmic extensions, and marginally wrinkled surface (Fig. 12A and B). The exposure of FB789 cells to NKL-WT (40 µM) specifically induced cell shrinkage and partial loss of substrate adhesion (Fig. 12C). Roundish or flatted shaped FB789 cells with squat extensions and plasma membrane rupture were observed after exposure to the highest NKL peptide concentration (80

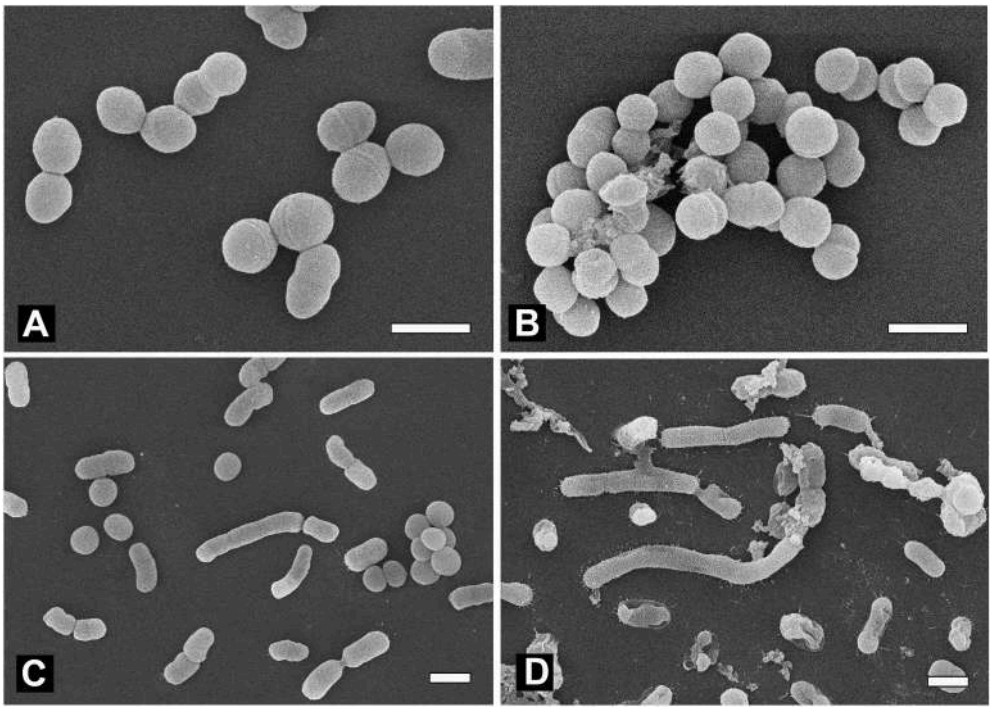

Fig. 10. A-D. SEM micrographs of *Enterococcus faecalis* and *Acinetobacter baumannii.* Untreated *E. faecalis* cells (A), *E. faecalis* cells treated with NKL-WT peptide (16 μg/ml, 5 μM) (B), untreated *A. baumannii* cells (C), *A. baumannii* after exposure to NKL-MUT peptide (32 μg/ml, 10 μM) (D). Scale bars = 1 μm.

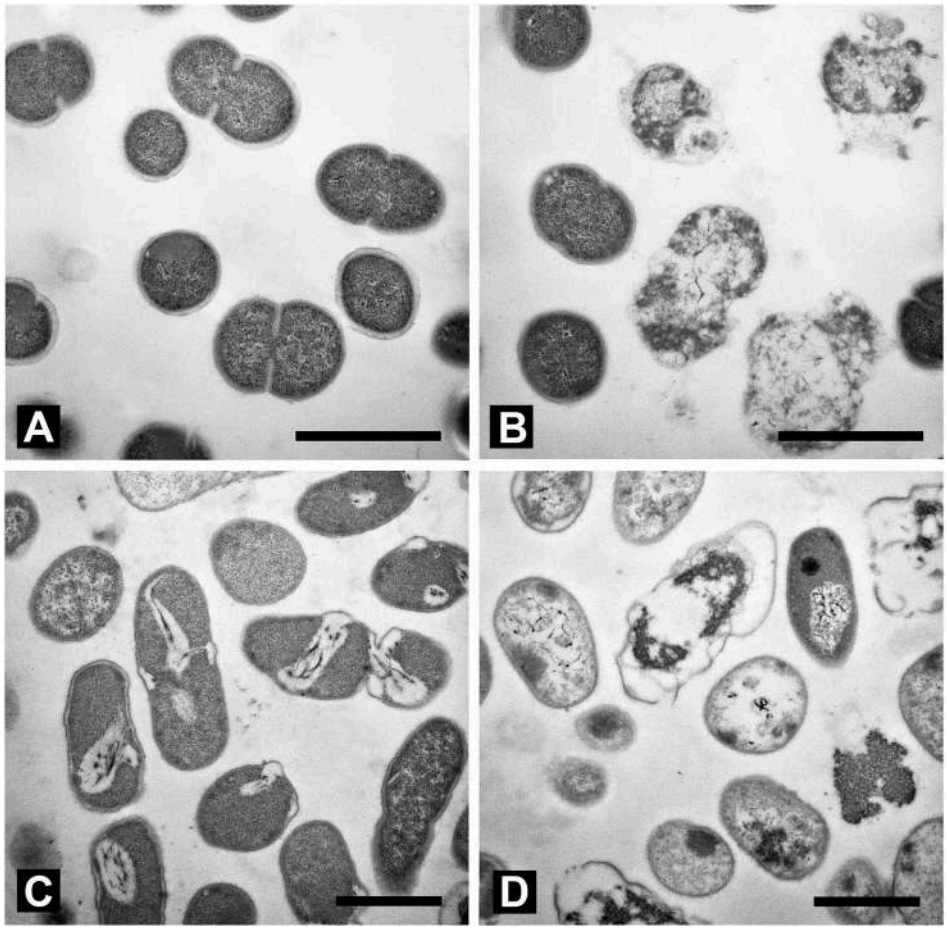

Fig. 11. A-D. TEM micrographs of *Enterococcus faecalis* and *Acinetobacter baumannii. E. faecalis* in standard medium (A), *E. faecalis* after incubation with NKL-WT (16 μg/ml, 5 μM) (B), untreated *A. baumannii* cells (C), *A. baumannii* cells after exposure to NKL-MUT (32 μg/ml, 10 μM) (D). Scale bars = 1 μm.

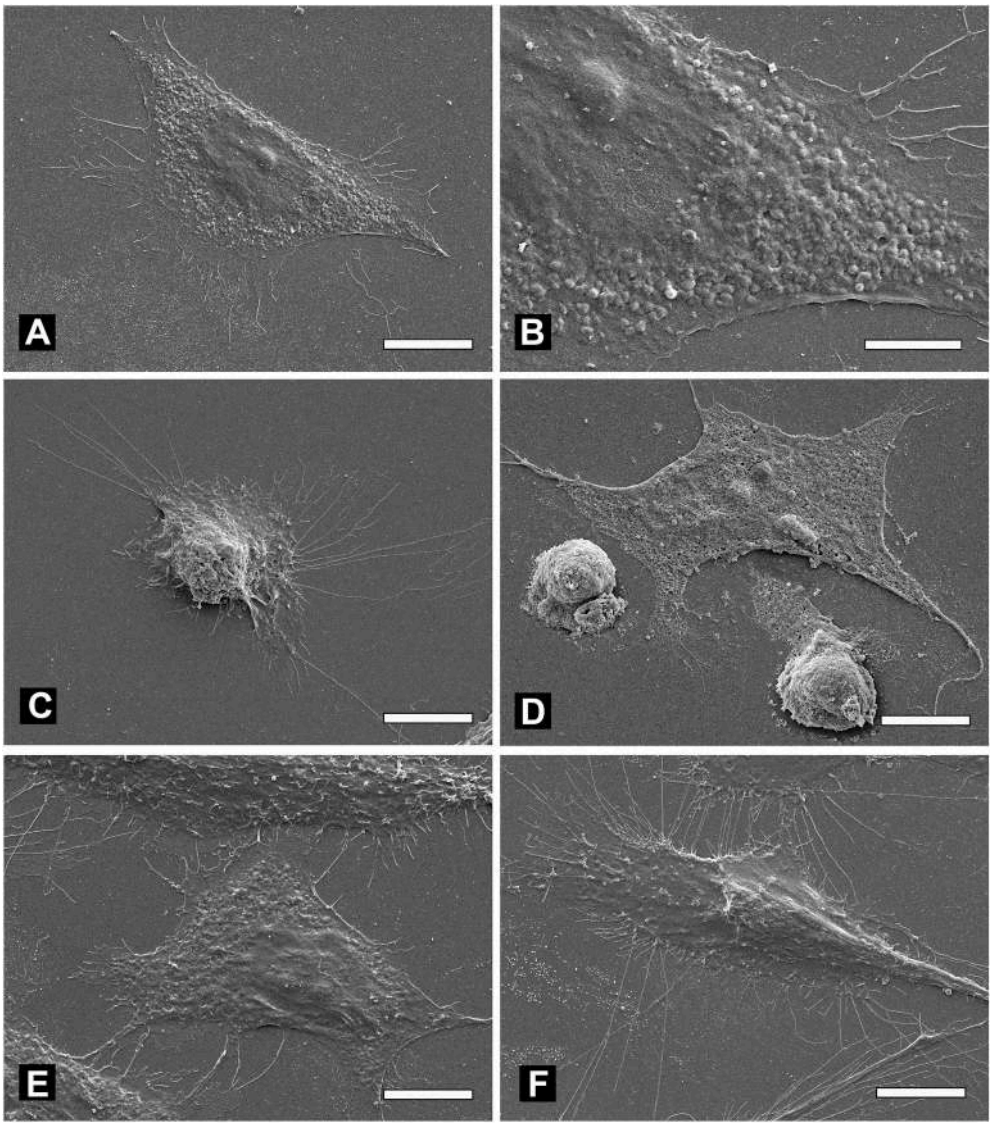

Fig. 12. A-F. SEM analysis of peptide-induced effects on human fibroblasts cell line (FB7689). Untreated FB789 cells (negative control) (A), and its higher magnification (B), FB789 cells exposed to 40 μM (C) and 80 μM NKL-WT (D), FB789 treated with 40 μM (E) and 80 μM NKL-MUT (F). Scale bars = A, C–F: 10 μm; B: 5 μm.

μM) (Fig. 12 D). Otherwise, fibroblasts (FB789) treated with the two highest concentrations of NKL-MUT peptide (40 μM and 80 μM) maintained control cell-like morphology (Fig. 12E and F).

Untreated B16F10 cells (negative control) appeared as fusiform shaped cells with numerous long cytoplasmic protrusions and corrugated plasma membrane (Fig. 13A and B). After exposure to NKL-WT (40 μM), B16F10 cells exhibited morphological changes such as cell shrinkage, roundish shape and reduced cytoplasmic protrusions (Fig. 13C). Roundish and flatted shaped cells, ruptures of cell membrane, loss of cytoplasmic protrusions and membrane blebs were observed in B16F10 cells exposed to the highest concentration of NKL-WT (80 μM) (Fig. 13 D). Moreover, B16F10 cells exposed to NKL-MUT peptide (40 μM) showed short cellular offshoots and plasma membrane blebbings, characterized by a spherical, bulky morphology (Fig. 13 E). The highest dose (80 μM) of NKL-MUT peptide further reduced cytoplasmic protrusions in B16F10 cells and increased the production of cell debris (apoptotic bodies) as a product of cell disassembly. Such cells exhibited roundish shape and numerous plasma membrane blebbings (Fig. 13 F).

3.10. Molecular dynamics simulations of NKL-WT and NKL-MUT in water

Molecular dynamics (MD) simulations of NKL-WT and NKL-MUT in water were conducted to investigate the effect of aa mutation on NKL structure. The analysis of the secondary structure of NKL-WT and NKL-MUT showed a higher content of α-helix in wild-type peptides (77%) with respect to mutant (49%) (Fig. 14 A and Fig. 14 B). In particular, in NKL-WT the residues between Leu-2 and Asn-11 on the N-terminal region and those between Leu-16 and Phe-23 on the C-terminal region adopt an α-helix structure for more than 70% of the simulation time (production phase) (Fig. 14C). The two α-helices were separated by a turn of three residues (Lys-12, Ile-13 and Gly-14) and the disulphide bond between the Cys-10 and Cys-20 constrains the peptide to adopt a stable U structure as it was found in the 3D structure of the full-length peptide (Fig. S1). In NKL-MUT only the residues of the C-terminal region, between Lys-12 and Lys-22, formed a stable α-helix structure for more than 80% of simulation time (Fig. 14 D). Fig. 14 E and F show the superimposition of the configurations, one structure per 2 ns of NKL-WT and NKL-MUT obtained in the last 300 ns of MD simulations. The peptide NKL-WT appeared to have a rigid structure with respect to the

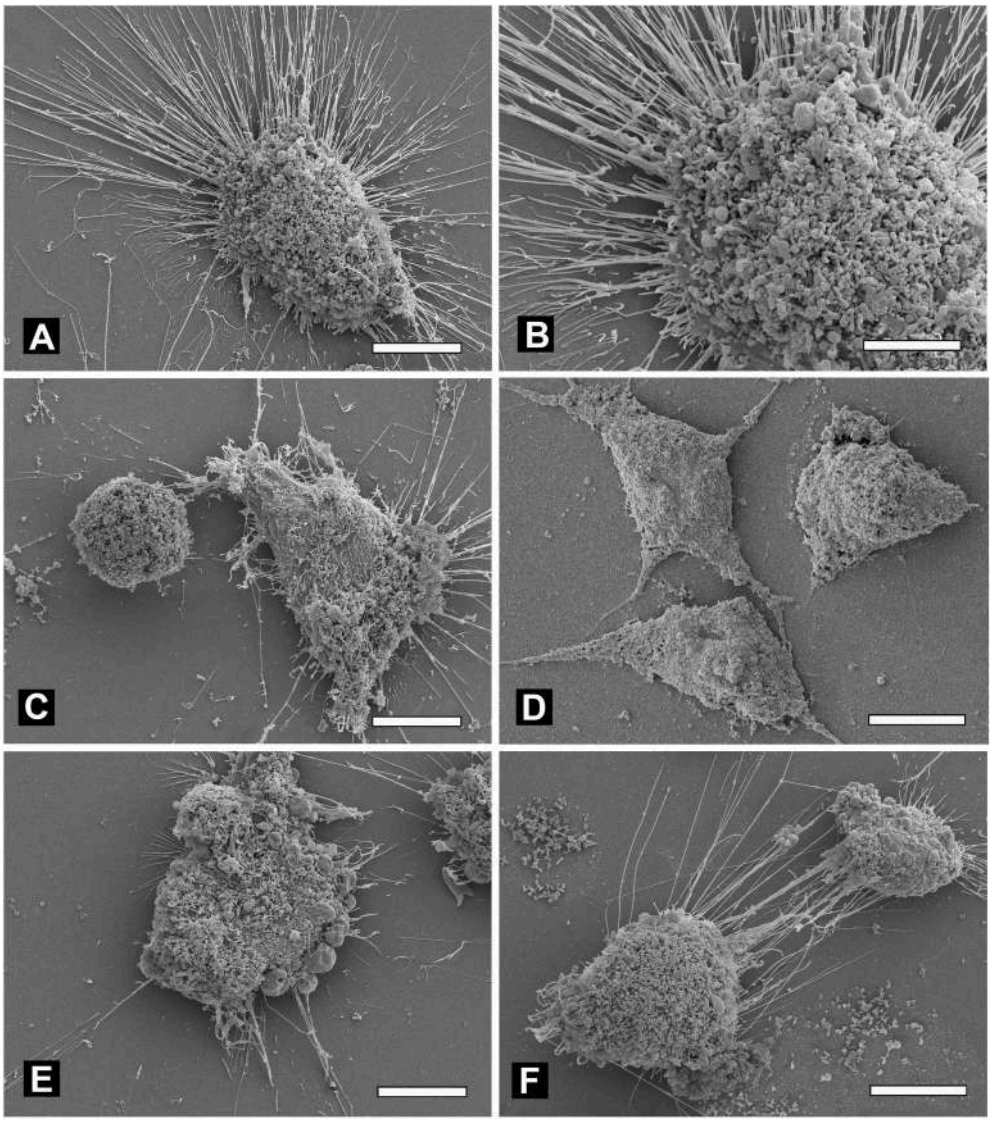

Fig. 13. A-F. SEM analysis of peptide-induced effects on murine melanoma cell line (B16F10). Untreated B16F10 cells (negative control) (A) and its higher magnification (B), B16F10 cells after exposure to 40 μM (C) and 80 μM NKL-WT (D), B16F10 cells treated with 40 μM (E) and 80 μM NKL-MUT (F). Scale bars = A, C–F: 10 μm; B: 5 μm.

mutant due to the presence of the disulphide bond that reduces the degree of conformational freedom of wild-type peptide. NKL-MUT showed a high degree of flexibility, the unstructured N-terminal region experiments, during the simulation, many possible conformations.

4. Discussion

Marine biodiversity is a gold and yet largely unexplored mine for the discovery of bioactive peptides [43]. Since marine organisms live in very dynamic, hostile and pathogen-rich environment, with high degree of competitiveness and antagonism between species, they have produced an astounding variety of host defence peptides with composition, sequence and structures different from the ones found in terrestrial species [44]. Among them, AMPs from fish are highly studied due to their involvement in the robust innate immune response of these vertebrates and to their direct antimicrobial potency against pathogens like bacteria, viruses, fungi, parasites and protozoans [45,46]). That is why fish AMPs have caught scientists' attention and are being investigated for their potential role in antimicrobial and therapeutic applications. Taking these considerations into account, we focused our attention on a NK-lysin peptide identified from *T. bernacchii*, a teleost fish belonging to the Notothenioidei suborder and living in a peculiar ecosystem, such as the Antarctic region. Antarctic Notothenioidei are the dominant fish group in the Southern Ocean. They have developed unique defences against the extreme environment leading to a diverse array of biochemical and physiological adaptations [47] and the ability to produce unique bioactive molecules. As an example, the trematocine peptide, belonging to the piscidin family, is active against both Gram+ (*Bacillus pumilus*) and Gram- (*Escherichia coli* and *Psychrobacter* sp. TAD 1) bacteria [23]. Herein, the putative mature NK-lysin amino acid sequence was identified in the *T. bernacchi* transcriptome [24,48]. The full precursor sequence is slightly longer compared to the corresponding peptides found in other fish species, although it contains six conserved cysteine residues into the typical saposin-like domain of these AMPs. As supported by structural modelling, these cysteines are likely involved in the formation of three disulfide bonds that in mammals are essential for achieving the characteristic NK-lysin tertiary structure comprehensive of five amphipathic α-helices [3]. Moreover, a possible signature relative to cold adaptation has been evidenced involving two amino acids of the mature peptide and, interestingly, one substitution was related to a charged one (lysin). NK-lysin mRNA was detected in all the examined immune-related tissues and organs of non-stimulated *T. bernacchii.* The

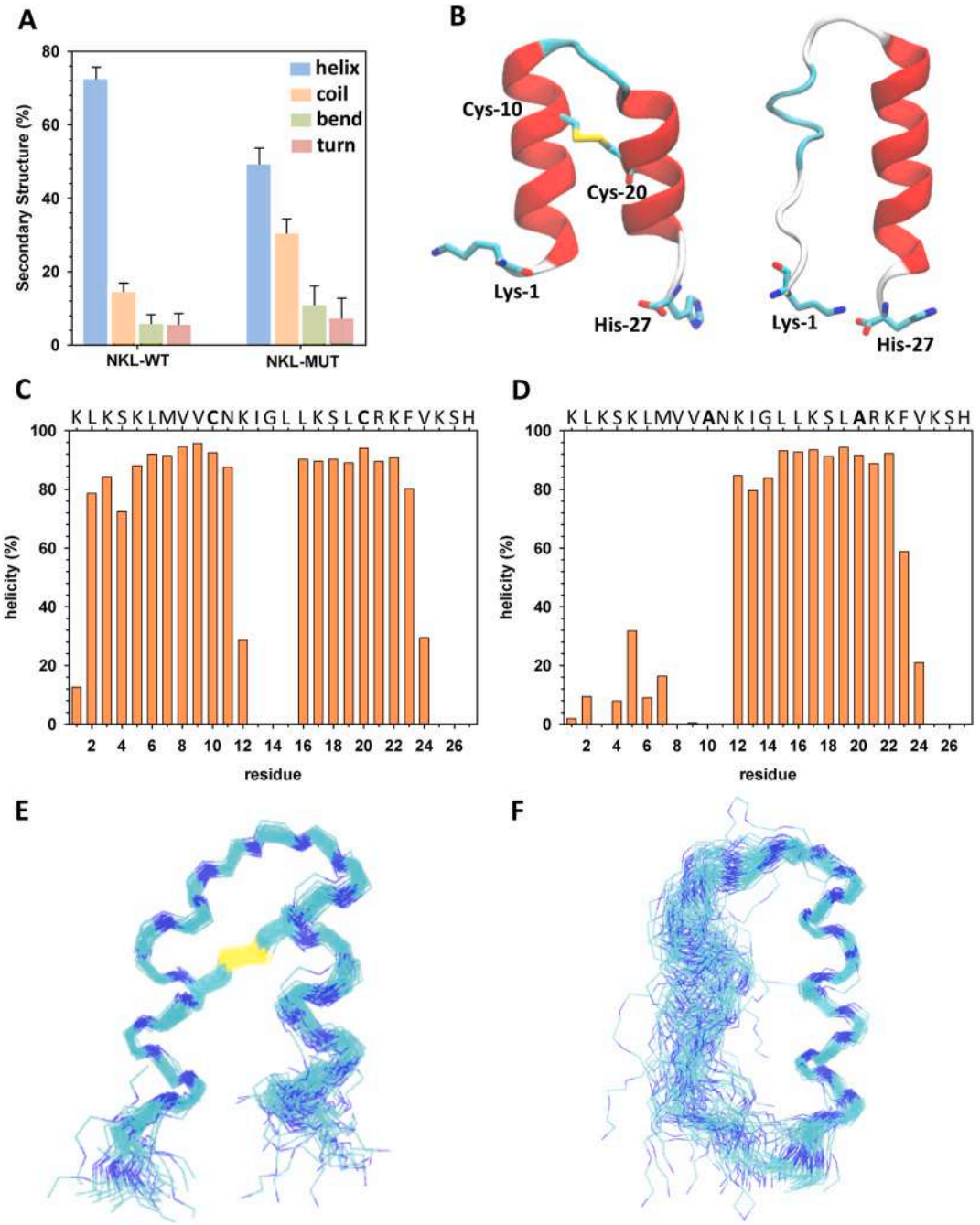

Fig. 14. Structural studies on peptides. **(**A) Percentage of secondary structure of NKL-WT and NKL-MUT calculated on the last 300 ns of MD simulations. (B) Snapshot of NKL-WT and NKL-MUT at the end of 500 ns of molecular dynamics simulations. The secondary structure of peptides is represented in new-cartoons and α--helix is coloured in red while the residue Lys-1, Cys-10, Cys-20 and His-27 are represented in stick. (C) helicity (defined as the percentage of simulation time that a residue forms α-helix) of NKL-WT, (D) helicity of NKL-MUT. (E) Superimposition of NKL-WT configuration during the MD simulation, one frame per 2 ns. (F) Superimposition of NKL-MUT configuration during the MD simulation, one frame per 2 ns.

highest gene expression was detected in gills, a mucosal barrier that in fish acts as first line of innate defence against invading organisms, and spleen, an important fish hematopoietic tissue [49]. A similar constitutive expression pattern was found in other fish species like yellow catfish [50], mudskipper [12], tilapia [15] and yellow croaker [11], although tissue-specific expression of NKLs may differ in different fish species. Relative lower expression of NK-lysin was quantified in head kidney, gut and liver. Notably, gills, head kidney, spleen and gut expression was significantly higher than brain and muscle, thus suggesting that *T. bernacchii* NK-lysin may be involved in host defence against pathogens, as recently reported in other teleost species [51,52].

After having confirmed that *T. bernacchii* NKL showed features of an antimicrobial peptide, its actual bioactivity was investigated. However, due to its large size, the entire mature peptide could not be produced by organic synthesis and, therefore, we produced a smaller region (27 aa-long) of the Saposin-like domain taking into account the potent biological activity exerted by the peptide NK-2 selected from human NK-lysin [6]. Considering that this sequence contained two cysteine residues that are involved in the formation of a disulphide bond in the full-length peptide this was included in the synthetic AMP (NKL-WT). A similar strategy was employed in a previous study concerning a teleost fish NK-lysin [12] to obtain a peptide with a 3D structure resembling

that of the naturally produced *in vivo* molecule**.** Moreover, a mutant molecule (NKL-MUT) with the two cysteines replaced by alanine residues was also produced to evaluate the effects of the formed covalent bond on the examined biological activity. Specifically in fish, NKLs are known to act as direct microbe-killing molecules [19,53]. Most cationic AMPs interact with negatively charged outer microbial membranes through electrostatic interactions [54], leading to membrane permeabilization, cellular lysis and death [55]. These steps define the molecular mechanism by which most membrane-active peptides lyse the membranes, although it is well known that others, typically highly charged peptides, show antimicrobial activity by targeting intracellular components without inducing direct membrane lytic mechanism [56]. To evaluate the ability of NKL-WT and NKL-MUT peptides to alter the bacterial membrane permeability, a membrane permeabilization assay was carried out using the fluorescent probe ANS [23]. To this purpose we considered the bacterial models *Escherichia coli* (Gram –) and *Bacillus cereus* (Gram +)*,* and, in addition, the Antarctic psychrotolerant bacterium *Psychrobacter* sp. TAD1. Based on the results, NKL-WT was highly and more effective against both *E. coli* and *B. cereus* (ANS uptake at 5 μM was 91% and 73%, respectively) compared to NKL-MUT (ANS uptake at 5 μM 50% and 42%, respectively). Both peptides exhibited a stronger membrane permeabilizing effect on *E. coli*. Notably, they were equally active against *Psychrobacter* sp. TAD1, an endemic bacterium from Antarctica. These results are in agreement with data obtained in golden pompano [13], black rockfish [14] and yellow catfish [50], and confirm the capacity of these peptides to target and permeabilize bacterial membranes. Since the ability to modulate the membrane permeability represents an important property of potential antimicrobial candidates, we tested the activity of both peptides against a panel of pathogen strains, with a focus on multi-drug resistant bacteria, such as ESKAPE isolates obtained from clinical isolates. Notably, the NKL-WT showed a low MIC value (16 μg/mL) against a Gram – strain, *Escherichia coli*, and against Gram + strains, *Enterococcus faecalis*, *Streptococcus pyogenes*, and *Staphylococcus capitis*. On the contrary, the NKL-MUT peptide was selective and highly active against the Gram-pathogens, *Acinetobacter baumannii*, *Escherichia coli* and *Klebsiella pneumoniae* (MIC 8 μg/mL, MIC 16 μg/mL, MIC 32 μg/mL, respectively). It is known in literature that some AMPs, preferentially acting against Gram-bacteria, seem to interact more strongly with zwitterionic phosphatidylethanolamine (PE), a phospholipid component present in high concentrations on Gram-bacteria's membrane, than negatively charged phosphatidylglycerol (PG) phospholipid [57]. The preferential interaction with PE could explain AMP preference against Gram-bacteria. Our data demonstrate that the peptide modification increases susceptibility against Gram-bacteria and optimises the selectivity of the molecule to interact with complex and specialised cell envelopes, that represent a relevant barrier making Gram-bacteria intrinsically resistant to many antibiotics [58]. Scanning electron microscopy (SEM) and transmission electron microscopy (TEM) were used to examine the ultrastructural changes in bacteria induced by NKL-WT and NKL-MUT, respectively. The representative Gram-strain, *A. baumanni*i, and the Gram + strain *E. faecalis* were exposed to NKL-WT and NKL-MUT peptides at MBC (16 μg/mL NKL-WT for *E. faecalis,* and 32 μg/mL NKL-MUT for *A. baumanni*i). SEM revealed significant morphological changes in both bacteria and the presence of dead cells; moreover, membrane breaks, release of cytoplasmic contents and evident morphological alterations in the DNA region were observed by TEM analysis. From these results, we can state that *A. baumannii* is susceptible to NK-MUT while *E. faecalis* to NK-WT. This is consistent with the evidence that most NK-lysin homologues identified from fish species show antibacterial activity against pathogens of pharmaceutical interest. As a result of the toxic action against bacteria, AMPs usually have highly associated haemolytic and/or cytotoxic activity at MIC value. The mammalian cell toxicity is a possible undesirable property and, particularly, the erythrocytes selectivity represents a challenge to consider when designing new AMPs [59]. In our study, NKL-WT and NKL-MUT did not show any haemolytic activity on erythrocytes, at their effective MIC and MBC values for *E. faecalis* and *A. baumannii*, respectively. Of note, NKL-MUT appeared to be a safe drug even when tested at supra-MIC and MBC values. As a consequence, the route of administration may not be restricted to topical use but to systemic application as well. This is an important goal of peptide design as currently there is a clear need for systemic antimicrobials to treat bloodstream infections caused by antibiotic-resistant pathogens [60].

Studies related to the use of AMPs from fish are being carried out to find an alternative cure for cancer [61,62] and NK-lysins from mammals are well known for their cytotoxic activity against tumoral cell lines. To achieve this objective, the AMPs employed must target tumour cells without affecting normal cells. NKL-MUT selectively targeted tumour cells promoting cancer cells apoptosis. Of note, it possessed improved cytotoxicity and higher pro-apoptotic activity compared to NKL-WT towards the tested melanoma cell line (B16F10), with no significant side effects on fibroblasts (FB789), at all the analysed concentrations. When exposed to melanoma cells, NKL-MUT induced DNA fragmentation and apoptosis*,* as documented by the presence of cell shrinkage, ruffling plasma membrane and breaking up of the cell fragments in apoptotic bodies. Moreover, secondary necrosis, a phenomenon referring to the progressive loss of plasma membrane integrity of apoptotic cells [63], was also observed in tumour cells. The mechanism underlying each peptide bioactivity depends on the peptide properties (amino acid residue composition, sequence length, molecular weight, isoelectric point, net charge, hydrophobicity, amphi-philicity, secondary structure in membrane, spatial structure and oligomerization ability) and on the characteristics of the target membrane, that promote or inhibit drug cell surface interaction and penetration [64]. The specific recognition of tumour cells is facilitated by the presence of negatively charged phosphatidylserine on their outer leaflet of plasma membrane [65,66]. Other features, such as lower cholesterol content, the presence of more abundant filopodia and microvilli on the tumour cells compared to healthy cell may enhance susceptibility to peptides and promote selective cytotoxicity [64]. The MD simulations of NKL-WT in water revealed a stable and rigid structure with two α-helices separated by a turn of three residues (Lys-12, Ile-13, and Gly-14) and the disulphide bond between the Cys-10 and Cys-20, that reduces the degree of conformational freedom. Otherwise, NKL-MUT showed a structure with a single α-helix and a region with a high degree of flexibility. The results obtained by the analysis of MD trajectories for NKL-WT and NKL-MUT highlight the key role of the disulphide bond between Cys-10 and Cys-20 to control the structure and dynamics of the natural and modified peptide, with important effects on and differences between their bioactivity, membrane interaction and cell selectivity.

In conclusion, the outcome of this study may be considered as a promising starting point for designing new candidate drugs and open up interesting perspectives for the possible application of the NK-lysin peptides in the pharmacological and biomedical fields.

Funding

This work was supported by the National Programme for Antarctic Research (PNRA) [Grant number PNRA18_00077].

CRediT authorship contribution statement

F. Buonocore: Conceptualization, Writing – original draft, Writing – review & editing. **P.R. Saraceni:** Investigation. **A.R. Taddei:** Investigation. **A. Miccoli:** Formal analysis, Data curation. **F. Porcelli:** Resources, Investigation. **S. Borocci:** Investigation. **M. Gerdol:** Resources. **F. Bugli:** Resources, Investigation. **M. Sanguinetti:** Resources. **A.M. Fausto:** Writing – review & editing. **G. Scapigliati:** Writing – review & editing. **S. Picchietti:** Conceptualization, Writing – original draft, Writing – review & editing, Supervision, Project administration, Funding acquisition.

Declaration of competing interest

All authors declare no conflict of interest.

Data availability

Data will be made available on request.

Acknowledgements

We thank Dr. Valentina Laghezza Masci for excellent technical assistance in flow cytometry analysis.

Appendix A. Supplementary data

Supplementary data to this article can be found online at https://doi.org/10.1016/j.fsi.2023.109099.

References

[1] M. Andersson, H. Gunne, B. Agerberth, A. Boman, T. Bergman, R. Sillard, H. Jörnvall, V. Mutt, B. Olsson, H. Wigzell, Å. Dagerlind, H.G. Boman, G. H. Gudmundsson, NK-lysin, a novel effector peptide of cytotoxic T and NK cells. Structure and cDNA cloning of the porcine form, induction by interleukin 2, antibacterial and antitumour activity, EMBO J. 14 (1995) 1615–1625, https://doi.org/10.1002/j.1460-2075.1995.tb07150.x.

[2] Y. Zhai, M.H. Saier, The amoebapore superfamily, Biochim. Biophys. Acta Rev. Biomembr. 1469 (2000) 87–99, https://doi.org/10.1016/S0304-4157(00)00003-4.

[3] E. Liepinsh, M. Andersson, J.M. Ruysschaert, G. Otting, Saposin fold revealed by the NMR structure of NK-lysin, Nat. Struct. Biol. 4 (1997) 793–795, https://doi.org/10.1038/nsb1097-793.

[4] M. Andersson, R. Girard, P.A. Cazenave, Interaction of NK lysin, a peptide produced by cytolytic lymphocytes, with endotoxin, Infect. Immun. 67 (1999) 201–205, https://doi.org/10.1128/iai.67.1.201-205.1999.

[5] J. Andrä, T. Gutsmann, P. Garidel, K. Brandenburg, Mechanisms of endotoxin neutralization by synthetic cationic compounds, J. Endotoxin Res. 12 (2006) 261–277, https://doi.org/10.1179/096805106x118852.

[6] J. Andrä, M.H.J. Koch, R. Bartels, K. Brandenburg, Biophysical characterization of endotoxin inactivation by NK-2, an antimicrobial peptide derived from mammalian NK-lysin, Antimicrob. Agents Chemother. 48 (2004) 1593–1599, https://doi.org/10.1128/AAC.48.5.1593-1599.2004.

[7] T. Jacobs, H. Bruhn, I. Gaworski, B. Fleischer, M. Leippe, NK-lysin and its shortened analog NK-2 exhibit potent activities against trypanosoma cruzi, Antimicrob. Agents Chemother. 47 (2003) 607–613, https://doi.org/10.1128/AAC.47.2.607-613.2003.

[8] Q. Wang, B. Bao, Y. Wang, E. Peatman, Z. Liu, Characterization of a NK-lysin antimicrobial peptide gene from channel catfish, Fish Shellfish Immunol. 20 (2006) 419–426, https://doi.org/10.1016/j.fsi.2005.05.005.

[9] I. Hirono, H. Kondo, T. Koyama, N.R. Arma, J.Y. Hwang, R. Nozaki, N. Midorikawa, T. Aoki, Characterization of Japanese flounder (Paralichthys olivaceus) NK-lysin, an antimicrobial peptide, Fish Shellfish Immunol. 22 (2007) 567–575, https://doi.org/10.1016/j.fsi.2006.08.003.

[10] M. Zhang, M.F. Li, L. Sun, NKLP27: a teleost NK-lysin peptide that modulates immune response, induces degradation of bacterial DNA, and inhibits bacterial and viral infection, PLoS One 9 (2014), https://doi.org/10.1371/journal.pone.0106543.

[11] Q.J. Zhou, J. Wang, M. Liu, Y. Qiao, W.S. Hong, Y.Q. Su, K.H. Han, Q.Z. Ke, W. Q. Zheng, Identification, expression and antibacterial activities of an antimicrobial peptide NK-lysin from a marine fish Larimichthys crocea, Fish Shellfish Immunol. 55 (2016) 195–202, https://doi.org/10.1016/j.fsi.2016.05.035.

[12] F.-F. Ding, C.-H. Li, J. Chen, Molecular characterization of the NK-lysin in a teleost fish, Boleophthalmus pectinirostris: antimicrobial activity and immunomodulatory activity on monocytes/macrophages, Fish Shellfish Immunol. 92 (2019) 256–264, https://doi.org/10.1016/j.fsi.2019.06.021.

[13] H. Zhang, Z. Cao, Q. Diao, Y. Zhou, J. Ao, C. Liu, Y. Sun, Antimicrobial activity and mechanisms of a derived antimicrobial peptide TroNKL-27 from golden pompano (Trachinotus ovatus) NK-lysin, Fish Shellfish Immunol. 126 (2022) 357–369, https://doi.org/10.1016/j.fsi.2022.05.052.

[14] D. Hao, G. Wang, N. Li, H. Liu, C. Wang, W. Liu, X. Yan, M. Zhang, Antimicrobial and immunoregulatory activities of the derived peptide of a natural killer lysin from black rockfish (Sebastes schlegelii), Fish Shellfish Immunol. 123 (2022) 369–380, https://doi.org/10.1016/j.fsi.2022.03.020.

[15] Y. Huang, Q. Zheng, J. Niu, J. Tang, B. Wang, E.D. Abarike, Y. Lu, J. Cai, J. Jian, NK-lysin from Oreochromis niloticus improves antimicrobial defence against bacterial pathogens, Fish Shellfish Immunol. 72 (2018) 259–265, https://doi.org/10.1016/j.fsi.2017.11.002.

[16] Z. hao Ruan, W. Huang, Y. fu Li, L. sen Jiang, Z. qiang Lu, Y. yuan Luo, X. quan Zhang, W. sheng Liu, The antibacterial activity of a novel NK-lysin homolog and its molecular characterization and expression in the striped catfish, Pangasianodon hypophthalmus, Fish Shellfish Immunol. 127 (2022) 256–263, https://doi.org/10.1016/j.fsi.2022.06.027.

[17] S.W. Luo, N.X. Xiong, Z.Y. Luo, L.F. Fan, K.K. Luo, Z.W. Mao, S.J. Liu, C. Wu, F. Z. Hu, S. Wang, M. Wen, A novel NK-lysin in hybrid crucian carp can exhibit cytotoxic activity in fish cells and confer protection against Aeromonas hydrophila infection in comparison with Carassius cuvieri and Carassius auratus red var, Fish Shellfish Immunol. 116 (2021) 1–11, https://doi.org/10.1016/j.fsi.2021.06.015.

[18] Y. Valero, C. González-Fernández, C. Cárdenas, F. Guzmán, R. León, A. Cuesta, NK-lysin peptides ameliorate viral encephalopathy and retinopathy disease signs and provide partial protection against nodavirus infection in European sea bass, Antivir. Res. 192 (2021), https://doi.org/10.1016/j.antiviral.2021.105104.

[19] A. Falco, R. Medina-Gali, J. Poveda, M. Bello-Perez, B. Novoa, J. Encinar, Antiviral activity of a turbot (Scophthalmus maximus) NK-lysin peptide by inhibition of low-pH virus-induced membrane fusion, Mar. Drugs 17 (2019) 87, https://doi.org/10.3390/md17020087.

[20] Y. Zhang, P. Deng, C. Dai, M. Wu, X. Liu, L. Li, X. Pan, J. Yuan, Investigation of putative antimicrobial peptides in Carassius gibel, revealing a practical approach to screening antimicrobials, Fish Shellfish Immunol. 121 (2022) 254–264, https://doi.org/10.1016/j.fsi.2021.12.050.

[21] R. Lama, P. Pereiro, M.M. Costa, J.A. Encinar, R.M. Medina-Gali, L. Pérez, J. Lamas, J. Leiro, A. Figueras, B. Novoa, Turbot (Scophthalmus maximus) Nk-lysin induces protection against the pathogenic parasite Philasterides dicentrarchi via membrane disruption, Fish Shellfish Immunol. 82 (2018) 190–199, https://doi.org/10.1016/j.fsi.2018.08.004.

[22] P. Pereiro, A. Romero, P. Díaz-Rosales, A. Estepa, A. Figueras, B. Novoa, Nucleated teleost erythrocytes play an nk-lysin- and autophagy-dependent role in antiviral immunity, Front. Immunol. 8 (2017), https://doi.org/10.3389/fimmu.2017.01458.

[23] G. Della Pelle, G. Perà, M.C. Belardinelli, M. Gerdol, M. Felli, S. Crognale, G. Scapigliati, F. Ceccacci, F. Buonocore, F. Porcelli, Trematocine, a novel antimicrobial peptide from the antarctic fish Trematomus bernacchii: identification and biological activity, Antibiotics 9 (2020) 66, https://doi.org/10.3390/antibiotics9020066.

[24] M. Gerdol, F. Buonocore, G. Scapigliati, A. Pallavicini, Analysis and characterization of the head kidney transcriptome from the Antarctic fish Trematomus bernacchii (Teleostea, Notothenioidea): a source for immune relevant genes, Mar. Genomics 20 (2015) 13–15, https://doi.org/10.1016/j.margen.2014.12.005.

[25] F. Teufel, J.J. Almagro Armenteros, A.R. Johansen, M.H. Gíslason, S.I. Pihl, K. D. Tsirigos, O. Winther, S. Brunak, G. von Heijne, H. Nielsen, SignalP 6.0 predicts all five types of signal peptides using protein language models, Nat. Biotechnol. 40 (2022) 1023–1025, https://doi.org/10.1038/s41587-021-01156-3.

[26] M. Mirdita, K. Schütze, Y. Moriwaki, L. Heo, S. Ovchinnikov, M. Steinegger, ColabFold: making protein folding accessible to all, Nat. Methods 19 (2022) 679–682, https://doi.org/10.1038/s41592-022-01488-1.

[27] M.W. Pfaffl, A new mathematical model for relative quantification in real-time RT-PCR, Nucleic Acids Res. 29 (2001) 2002–2007, https://doi.org/10.1093/nar/29.9.e45.

[28] C. Olivieri, F. Bugli, G. Menchinelli, G. Veglia, F. Buonocore, G. Scapigliati, V. Stocchi, F. Ceccacci, M. Papi, M. Sanguinetti, F. Porcelli, Design and characterization of chionodracine-derived antimicrobial peptides with enhanced activity against drug-resistant human pathogens, RSC Adv. 8 (2018) 41331–41346, https://doi.org/10.1039/C8RA08065H.

[29] EUCAST, The European Committee on Antimicrobial Susceptibility Testing, Breakpoint tables for interpretation of MICs and zone diameters, Version 13.1, 2023, https://www.eucast.org/, 2023.

[30] Y. Zhang, I-TASSER server for protein 3D structure prediction, BMC Bioinf. 9 (2008) 40, https://doi.org/10.1186/1471-2105-9-40.

[31] M.J. Abraham, T. Murtola, R. Schulz, S. Páll, J.C. Smith, B. Hess, E. Lindahl, GROMACS: high performance molecular simulations through multi-level parallelism from laptops to supercomputers, SoftwareX 1–2 (2015) 19–25, https://doi.org/10.1016/j.softx.2015.06.001.

[32] J. Huang, A.D. MacKerell, CHARMM36 all-atom additive protein force field: validation based on comparison to NMR data, J. Comput. Chem. 34 (2013) 2135–2145, https://doi.org/10.1002/jcc.23354.

[33] W.L. Jorgensen, J. Chandrasekhar, J.D. Madura, R.W. Impey, M.L. Klein, Comparison of simple potential functions for simulating liquid water, J. Chem. Phys. 79 (1983) 926–935, https://doi.org/10.1063/1.445869.

[34] T. Darden, D. York, L. Pedersen, Particle mesh Ewald: an N ·log(N) method for Ewald sums in large systems, J. Chem. Phys. 98 (1993) 10089–10092, https://doi.org/10.1063/1.464397.

[35] B. Hess, P-LINCS: a parallel linear constraint solver for molecular simulation, J. Chem. Theor. Comput. 4 (2008) 116–122, https://doi.org/10.1021/ct700200b.

[36] S. Miyamoto, P.A. Kollman, Settle: an analytical version of the SHAKE and RATTLE algorithm for rigid water models, J. Comput. Chem. 13 (1992) 952–962, https://doi.org/10.1002/jcc.540130805.

[37] G. Bussi, D. Donadio, M. Parrinello, Canonical sampling through velocity rescaling, J. Chem. Phys. 126 (2007), https://doi.org/10.1063/1.2408420.

[38] H.J.C. Berendsen, J.P.M. Postma, W.F. van Gunsteren, A. DiNola, J.R. Haak, Molecular dynamics with coupling to an external bath, J. Chem. Phys. 81 (1984) 3684–3690, https://doi.org/10.1063/1.448118.

[39] M. Parrinello, A. Rahman, Polymorphic transitions in single crystals: a new molecular dynamics method, J. Appl. Phys. 52 (1981) 7182–7190, https://doi.org/10.1063/1.328693.

[40] W. Humphrey, A. Dalke, K. Schulten, VMD: visual molecular dynamics, J. Mol. Graph. 14 (1996) 33–38, https://doi.org/10.1016/0263-7855(96)00018-5.

[41] W. Kabsch, C. Sander, Dictionary of protein secondary structure: pattern recognition of hydrogen-bonded and geometrical features, Biopolymers 22 (1983) 2577–2637, https://doi.org/10.1002/bip.360221211.
[42] A.-B. Schäfer, M. Wenzel, A how-to guide for mode of action analysis of antimicrobial peptides, Front. Cell. Infect. Microbiol. 10 (2020), https://doi.org/10.3389/fcimb.2020.540898.
[43] C. Mora, D.P. Tittensor, S. Adl, A.G.B. Simpson, B. Worm, How many species are there on earth and in the ocean? PLoS Biol. 9 (2011), e1001127 https://doi.org/10.1371/journal.pbio.1001127.
[44] M.W.F.S. Macedo, N.B. da Cunha, J.A. Carneiro, R.A. da Costa, S.A. de Alencar, M. H. Cardoso, O.L. Franco, S.C. Dias, Marine organisms as a rich source of biologically active peptides, Front. Mar. Sci. 8 (2021), https://doi.org/10.3389/fmars.2021.667764.
[45] Y. Valero, M. Saraiva-Fraga, B. Costas, F.A. Guardiola, Antimicrobial peptides from fish: beyond the fight against pathogens, Rev. Aquacult. 12 (2020) 224–253, https://doi.org/10.1111/raq.12314.
[46] U. Shabir, S. Ali, A.R. Magray, B.A. Ganai, P. Firdous, T. Hassan, R. Nazir, Fish antimicrobial peptides (AMP's) as essential and promising molecular therapeutic agents: a review, Microb. Pathog. 114 (2018) 50–56, https://doi.org/10.1016/j.micpath.2017.11.039.
[47] I. Bista, J.M.D. Wood, T. Desvignes, S.A. McCarthy, M. Matschiner, Z. Ning, A. Tracey, J. Torrance, Y. Sims, W. Chow, M. Smith, K. Oliver, L. Haggerty, W. Salzburger, J.H. Postlethwait, K. Howe, M.S. Clark, H. William Detrich, C.-H. Christina Cheng, E.A. Miska, R. Durbin, Genomics of cold adaptations in the Antarctic notothenioid fish radiation, Nat. Commun. 14 (2023) 3412, https://doi.org/10.1038/s41467-023-38567-6.
[48] T.J. Huth, S.P. Place, De novo assembly and characterization of tissue specific transcriptomes in the emerald notothen, Trematomus bernacchii, BMC Genom. 14 (2013) 805, https://doi.org/10.1186/1471-2164-14-805.
[49] H. Bjørgen, E.O. Koppang, Anatomy of teleost fish immune structures and organs, Immunogenetics 73 (2021) 53–63, https://doi.org/10.1007/s00251-020-01196-0.
[50] R. Zhu, Y.-S. Wu, X.-X. Liu, X. Lv, Y.-Q. Wu, J.-J. Song, X.-G. Wang, Membrane disruptive antimicrobial potential of NK-lysin from yellow catfish (Pelteobagrus fulvidraco), Fish Shellfish Immunol. 97 (2020) 571–580, https://doi.org/10.1016/j.fsi.2019.10.046.
[51] Y. Valero, E. Chaves-Pozo, A. Cuesta, NK-lysin is highly conserved in European sea bass and gilthead seabream but differentially modulated during the immune response, Fish Shellfish Immunol. 99 (2020) 435–441, https://doi.org/10.1016/j.fsi.2020.02.049.
[52] H. Xu, Z. Yuan, L. Sun, A non-canonical teleost NK-lysin: antimicrobial activity via multiple mechanisms, Int. J. Mol. Sci. 23 (2022), 12722, https://doi.org/10.3390/ijms232112722.
[53] Q.-J. Zhou, J. Wang, Y. Mao, M. Liu, Y.-Q. Su, Q.-Z. Ke, J. Chen, W.-Q. Zheng, Molecular structure, expression and antibacterial characterization of a novel antimicrobial peptide NK-lysin from the large yellow croaker Larimichthys crocea, Aquaculture 500 (2019) 315–321, https://doi.org/10.1016/j.aquaculture.2018.10.012.
[54] A. Hollmann, M. Martinez, P. Maturana, L.C. Semorile, P.C. Maffia, Antimicrobial peptides: interaction with model and biological membranes and synergism with chemical antibiotics, Front. Chem. 6 (2018), https://doi.org/10.3389/fchem.2018.00204.
[55] J.K. Boparai, P.K. Sharma, Mini review on antimicrobial peptides, sources, mechanism and recent applications, protein pept, Letture 27 (2019) 4–16, https://doi.org/10.2174/0929866526666190822165812.
[56] M.-A. Sani, F. Separovic, How membrane-active peptides get into lipid membranes, Acc. Chem. Res. 49 (2016) 1130–1138, https://doi.org/10.1021/acs.accounts.6b00074.
[57] A. Barreto-Santamaría, H. Curtidor, G. Arévalo-Pinzón, C. Herrera, D. Suárez, W. H. Pérez, M.E. Patarroyo, A new synthetic peptide having two target of antibacterial action in E. coli ML35, Front. Microbiol. 7 (2016), https://doi.org/10.3389/fmicb.2016.02006.
[58] A. Barreto-Santamaría, G. Arévalo-Pinzón, M.A. Patarroyo, M.E. Patarroyo, How to combat gram-negative bacteria using antimicrobial peptides: a challenge or an unattainable goal? Antibiotics 10 (2021) 1499, https://doi.org/10.3390/antibiotics10121499.
[59] M.N. Melo, R. Ferre, M.A.R.B. Castanho, Antimicrobial peptides: linking partition, activity and high membrane-bound concentrations, Nat. Rev. Microbiol. 7 (2009) 245–250, https://doi.org/10.1038/nrmicro2095.
[60] G. Wang, A.F. Mechesso, Realistic and Critical Review of the State of Systemic Antimicrobial Peptides, ADMET DMPK, 2022, https://doi.org/10.5599/admet.1215.
[61] A.A. Najm, A. Azfaralarriff, H.R. Eziwar Dyari, S.S. Syed Alwi, N. Khalili, B. A. Othman, D. Law, M. Shahid, S. Fazry, A systematic review of antimicrobial peptides from fish with anticancer properties, Pertanika J. Sci. Technol. 30 (2022) 1171–1196, https://doi.org/10.47836/pjst.30.2.18.
[62] P.J. Singh, A. Batta, S.K. Srivastava, Prospecting of Anti-Cancer Peptides (ACPs) from proteome of muscle tissue from Indian walking catfish, Clarias magur (Hamilton 1822) by Mass spectrometry and in silico approaches, Food Chem. Adv. 2 (2023), 100200, https://doi.org/10.1016/j.focha.2023.100200.
[63] C. Pfeffer, A. Singh, Apoptosis: a target for anticancer therapy, Int. J. Mol. Sci. 19 (2018) 448, https://doi.org/10.3390/ijms19020448.
[64] P.A. Trinidad-Calderón, C.D. Varela-Chinchilla, S. García-Lara, Natural peptides inducing cancer cell death: mechanisms and properties of specific candidates for cancer therapeutics, Molecules 26 (2021) 7453, https://doi.org/10.3390/molecules26247453.
[65] M.R. Felício, O.N. Silva, S. Gonçalves, N.C. Santos, O.L. Franco, Peptides with dual antimicrobial and anticancer activities, Front. Chem. 5 (2017), https://doi.org/10.3389/fchem.2017.00005.
[66] W. Chiangjong, S. Chutipongtanate, S. Hongeng, Anticancer peptide: physicochemical property, functional aspect and trend in clinical application (Review), Int. J. Oncol. 57 (2020) 678–696, https://doi.org/10.3892/ijo.2020.5099.